Su, J., Satchell, S. C., Wertheim, J. A., & Shah, R. N. (2019). Poly(ethylene glycol)-crosslinked gelatin hydrogel substrates with conjugated bioactive peptides influence endothelial cell behavior. *Biomaterials*, *201*, 99-112. https://doi.org/10.1016/j.biomaterials.2019.02.001

Title: **Poly(Ethylene Glycol)-Crosslinked Gelatin Hydrogel Substrates with Conjugated Bioactive Peptides Influence Endothelial Cell Behavior**

Authors: **Jimmy Su**[1,2,3], **Simon C. Satchell**[4], **Jason A. Wertheim**[1,2,3,5,6,7,†], **Ramille N. Shah**[1,2,8,†]

[1]Department of Biomedical Engineering, Northwestern University, Evanston, IL, USA
[2]Simpson Querrey Institute, Northwestern University, Chicago, IL, USA
[3]Comprehensive Transplant Center, Northwestern University Feinberg School of Medicine, Chicago, IL, USA
[4]Bristol Renal, University of Bristol, Dorothy Hodgkin Building, Bristol, United Kingdom
[5]Department of Surgery, Northwestern University Feinberg School of Medicine, Chicago, IL, USA
[6]Chemistry of Life Processes Institute, Northwestern University, Evanston, IL, USA
[7]Department of Surgery, Jesse Brown VA Medical Center, Chicago, IL, USA
[8]Department of Bioengineering, University of Illinois at Chicago, Chicago, IL, USA
[†]Corresponding Authors

Jason A. Wertheim, MD, PhD
676 N. St. Clair St., Suite 1900
Chicago, IL 60611
+1 (312) 695-0257
Jason.Wertheim@northwestern.edu

Ramille N. Shah, PhD
851 S. Morgan St., 2nd Fl.
Chicago, IL 60607
+1 (847) 609-2453
Ramille@uic.edu

Abstract

The basement membrane is a specialized extracellular matrix substrate responsible for support and maintenance of epithelial and endothelial structures. Engineered basement membrane-like hydrogel systems have the potential to advance understanding of cell-cell and cell-matrix interactions by allowing precise tuning of the substrate or matrix biochemical and biophysical properties. In this investigation, we developed tunable hydrogel substrates with conjugated bioactive peptides to modulate cell binding and growth factor signaling by endothelial cells. Hydrogels were formed by employing a poly(ethylene glycol) crosslinker to covalently crosslink gelatin polymers and simultaneously conjugate laminin-derived YIGSR peptides or vascular endothelial growth factor (VEGF)-mimetic QK peptides to the gelatin. Rheological characterization revealed rapid formation of hydrogels with similar stiffnesses across tested formulations, and swelling analysis demonstrated dependency on peptide and crosslinker concentrations in hydrogels. Levels of phosphorylated VEGF Receptor 2 in cells cultured on hydrogel substrates revealed that while human umbilical vein endothelial cells (HUVECs) responded to both soluble and conjugated forms of the QK peptide, conditionally-immortalized human glomerular endothelial cells (GEnCs) only responded to the conjugated presentation of the peptide. Furthermore, whereas HUVECs exhibited greatest upregulation in gene expression when cultured on YIGSR- and QK-conjugated hydrogel substrates after 5 days, GEnCs exhibited greatest upregulation when cultured on Matrigel control substrates at the same time point. These results indicate that conjugation of bioactive peptides to these hydrogel substrates significantly influenced endothelial cell behavior in cultures but with differential responses between HUVECs and GEnCs.

Keywords: Hydrogels, Peptides, YIGSR, QK, Basement Membrane

I. Introduction

The extracellular matrix (ECM) is composed of proteins, polysaccharides, and other biological molecules secreted by resident cells. These components together act as a natural scaffolding material that imparts mechanical integrity to tissues and organs as well as presents bioactive signals essential for cell and tissue development and maintenance[1, 2]. The ECM is a dynamic and highly-hydrated network akin to a stimulus-responsive hydrogel that is tailored to the microenvironmental needs of the inhabiting cells[3, 4]. In particular, the basement membrane (BM) is a specialized ECM substrate that lies beneath epithelial and endothelial cell populations and provides structural support, spatial organization, and bioactive signaling cues to the overlying cells[5]. Despite the popularity of naturally-derived materials such as basement membrane extracts (*e.g.*, Matrigel) for studying complex cell-cell and cell-matrix interactions, often times these materials are limited by lot-to-lot variability and the inability to precisely tune material properties[6].

The objective of this investigation was to engineer a hydrogel substrate capable of mimicking properties of the BM specifically to explore endothelial cell-cell and cell-matrix interactions. To accomplish this, we employed a versatile approach to generate hydrogels from both synthetic and natural polymer sources with tunable stiffness, termed the PEGX method[7]. The method utilizes a poly(ethylene glycol) (PEG) crosslinker, or PEGX, to form covalent crosslinks between available reactive groups on the polymers resulting in a stable network and hydrogel formation. Hydrogel stiffness may be modulated by varying the polymer concentration or the amount of crosslinker added, and the crosslinking method can be extended to a variety of different physical and chemical PEGX variants[7].

Gelatin was chosen as the base polymer for the hydrogels. Though not generally considered a BM component, gelatin is an accessible and economical biomaterial that has been employed in numerous biomedical applications, such as vehicles for drug delivery, scaffolds for tissue engineering, and hydrogels for 3D matrix cultures[8-10]. Because gelatin is derived from collagen, it retains key bioactive peptide sequences such as cell-binding sites (*e.g.*, RGD) and matrix metalloproteinase-sensitive degradation motifs. To specifically tailor the bioactivity of these hydrogel substrates to better mimic the BM of endothelial cells, we sought to incorporate peptide sequences known to modulate endothelial cell behavior. We further hypothesized that the desired peptides could be conjugated to the gelatin polymer through the use of additional PEGX, resulting in a covalent link that would lead to prolonged residence time, as opposed to simple encapsulation of the peptides within the hydrogels, and therefore extend availability for signaling pathway activation. Two peptides of significant interest for examining the effects on endothelial cells are the laminin-derived YIGSR peptide and the vascular endothelial growth factor (VEGF)-mimetic QK peptide.

The YIGSR peptide is derived from the β1 chain of laminin, a major component of the BM[5], and was discovered to mediate cell adhesion and migration through binding of the 67-kDa laminin receptor[11, 12]. Research by other groups demonstrated that modification of polyurethaneurea films and scaffolds with YIGSR peptides enhanced endothelial attachment and reduced platelet adhesion[13-15]. Interestingly, in combination with RGD peptides, YIGSR peptides inhibited endothelial growth on self-assembled peptide hydrogels[16]. However, additional investigations showed that covalent attachment of RGD and YIGSR peptides to PEG acrylate/diacrylate hydrogels enhanced endothelial cell migration[17] and tubulogenesis[18].

The QK peptide is a VEGF-mimetic peptide first designed by D'Andrea, *et al*. and confirmed to bind and activate VEGF Receptor 1 (VEGFR1 or Flt-1) and VEGF Receptor 2 (VEGFR2 or KDR)[19]. VEGF signaling is important in a variety of physiological contexts, but it is especially

critical in the development of new blood vessels and maintenance of healthy vasculature and endothelial function[20]. Furthermore, heparan sulfate proteoglycans, another major component of the BM, are known to bind and sequester growth factors including specific VEGF isoforms[5]. However, in contrast to large growth factors such as recombinant VEGF, the use of short, bioactive peptide mimetics is advantageous due to their smaller size, decreased chemical complexity, and reduced production costs[21]. The QK peptide consists of 15 natural amino acids and is likely named for the first and last residues that constitute the peptide's helical region (the sequence between residues 4 and 12 of the peptide) and correspond to the α-helix region of VEGF[19]. Research by other groups demonstrated that the QK peptide stimulated endothelial growth when tethered to elastin-like peptide hydrogels[22], promoted endothelial network formation when incorporated into type I collagen coatings[23], and enhanced endothelial tube-like structure formation when conjugated to PEG diacrylate[24] and gelatin methacrylate[25] hydrogels.

In this work, we developed crosslinked gelatin hydrogels with conjugated YIGSR and QK peptides using the PEGX method and evaluated these hydrogels as BM-like substrates for endothelial cell culture. Successful crosslinking of the gelatin polymers and conjugation of the YIGSR and QK peptides was determined by measuring the available reactive groups remaining after the crosslinking reaction. Rheology was performed to observe hydrogel crosslinking kinetics and measure the rheological properties (*i.e.*, shear moduli) of the hydrogels. Scanning electron microscopy and swelling analysis revealed the ultrastructural and swelling characteristics of the hydrogels, respectively. For cell culture studies, we employed human umbilical vein endothelial cells (HUVECs) and conditionally-immortalized human glomerular endothelial cells (GEnCs). Intracellular levels of phosphorylated VEGFR2 in response to treatment with soluble QK peptide or culture on QK-conjugated hydrogels was measured to assess the bioactivity of the peptide. Finally, gene expression of cells cultured on hydrogel substrates was evaluated at multiple timepoints.

II. Material & Methods

2.1. Peptide Synthesis and Determination of Peptide Concentrations for Experiments

QK, YIGSR, and RYGSI (scrambled YIGSR peptide control) peptides were purchased through custom peptide synthesis from ABI Scientific and confirmed to have a purity of >95% by high-performance liquid chromatography. Peptide sequences are listed in **Table 1**. Lysine ε-amino groups were acetylated to prevent cross-reactivity with the amine-reactive PEGX. C-termini of peptides were amidated to enhance stability, but N-termini were left unmodified. Peptides were solubilized in 1× phosphate-buffered saline solution (PBS, pH 7.4, Gibco, #10010) as concentrated stock solutions and frozen in aliquots at -20 °C. Aliquots were thawed and diluted as necessary for hydrogel preparation. Hydrogel formulations containing a range of peptide concentrations (QK and/or YIGSR) were devised based on evaluations of literature investigations. Previous studies exploring the bioactivity of the QK peptide and incorporation of the QK peptide into other hydrogel systems tested concentrations ranging from 1 µM to 100 µM and greater[19, 23-25]. Therefore, we selected QK peptide concentrations of 0, 1, 10, and 100 µM to evaluate its effect on endothelial cells when conjugated to hydrogels using the PEGX method. A study investigating conjugation of the YIGSR peptide into PEG diacrylate hydrogels used a concentration of 3.5 mM[18]. Another study incorporating the YIGSR peptide into self-assembling peptide hydrogels found optimal HUVEC growth at a concentration of 6 mM[16]. Therefore, we selected YIGSR concentrations of 0, 3, 6, and 12 mM to evaluate its effect on endothelial cells when conjugated to hydrogels using the PEGX method.

Table 1: Peptide Sequences

Peptide	Sequence (N-terminal to C-terminal)	Theoretical MW (g/mol)
QK	(K-Ac)LTWQELYQL(K-Ac)Y(K-Ac)GI where (K-Ac) indicates acetylation of the lysine ε-amino group	2036.31
YIGSR	YIGSR	593.68
RYGSI	RYGSI	593.68

2.2. Preparation of Hydrogels and Phase Analysis

The general strategy for the preparation of PEG-crosslinked gelatin hydrogels with conjugated peptides is outlined in **Scheme 1**. Gelatin type A (Sigma, #G1890) was solubilized in PBS at 37 °C at a stock concentration of 10% (m/v). Hydrogel precursor polymer solutions were prepared by mixing the following in order: PBS for dilution, 1 M NaOH (Sigma, #S2770) to buffer solutions to an approximate final pH of 6 for optimal crosslinking kinetics, peptides (if desired), and gelatin stock solution. Polymer solutions were held at 37 °C prior to crosslinking to ensure solution phase and thoroughly vortexed before the addition of crosslinker. Homobifunctional poly(ethylene glycol) succinimidyl valerate (SVA) (MW 5000 g/mol, Laysan Bio), referred to as simply PEG crosslinker or PEGX, was prepared as a concentrated stock solution at 40 mM in PBS just prior to crosslinking of polymer solutions. Immediately after adding PEGX to hydrogel precursor polymer solutions, solutions were vortexed, pipetted into well plates or molds as necessary, and incubated at 37 °C for 2 hrs. Main hydrogel formulations investigated are listed in **Table 2**. For phase analysis and phase plot generation, hydrogel formulations were prepared in microcentrifuge tubes. After the 2 hr incubation period, phase of formulations, either solution (sol) or hydrogel (gel), was determined by tube inversion, and those determined to be gel phase were manipulated with a spatula to qualitatively gauge hydrogel stiffness. Hydrogels that could be easily spread were designated as "soft", and those that retained their shape were designated as "robust"[7].

Table 2: Main Hydrogel Formulations Tested

Sample	No Peptides	QK	YIGSR	YIGSR/QK	RYGSI (Scrambled YIGSR Control)
Gelatin, % (m/v)	5.0	5.0	5.0	5.0	5.0
QK (μM)	0.0	100.0	0.0	100.0	0.0
YIGSR (mM)	0.0	0.0	12.0	12.0	0.0
RYGSI (mM)	0.0	0.0	0.0	0.0	12.0
PEGX (mM)	1.55	1.60	7.95	8.00	7.95
PEGX:Gelatin (m:m)	0.155	0.160	0.795	0.800	0.795

2.3. Quantification of Free Amine Content

Free amine content of hydrogel precursor polymer solutions and crosslinked hydrogels were quantified by the 2,4,6-trinitrobenzenesulfonic acid (TNBS) assay and performed according to previously published studies[7, 26, 27]. TNBS working solution was prepared fresh by diluting stock solution (picrylsulfonic acid solution, Sigma, #P2297) to a concentration of 0.01 M with a 4% (m/v) sodium bicarbonate solution (Sigma, #S5761), pH 8.5 prepared in deionized H_2O. A volume of 500 μL TNBS working solution was added to freshly-prepared 50-μL hydrogel precursor polymer solutions and crosslinked hydrogels, and samples were incubated at 37 °C for 2 hrs. To stop reactions, 500 μL of 10% (m/v) sodium dodecyl sulfate (Sigma, #L3771) prepared in deionized H_2O and 250 μL of 1 M HCl (Sigma, #H9892) were added to samples. Samples were then allowed to hydrolyze overnight at 37 °C. Samples were diluted as necessary in deionized H_2O, and 200

µL per sample was transferred to a clear 96-well plate. Absorbance at 335 nm (A_{335}) was measured on a BioTek Cytation 3 Cell-Imaging Multi-Mode Reader. Samples were tested in triplicate (n = 3) with technical replicates in duplicate, compared to a standard curve of L-leucine (Sigma, #L8000), and normalized to the uncrosslinked control group of 5% (m/v) gelatin solution with no peptides.

2.4. Rheological Characterization and pH Measurement

Rheological characterization of hydrogels was performed following a recommended protocol for hydrogels for tissue engineering applications[28]. Testing was performed using an Anton Paar MCR 302 rheometer with a 25-mm 2°-angle cone-plate fixture under strain-controlled conditions. The lower Peltier cell was set to 37 °C and allowed to equilibrate prior to sample loading. All samples were mixed fresh and immediately loaded onto the rheometer stage. Once the measuring system was lowered, mineral oil (Amresco, #J217) was applied to the edges of the fixture and sample, and the entire system was enclosed within a solvent trap to prevent sample dehydration. Time sweeps were performed for 2 hrs at 37 °C, 1% strain, and 10 rad/s. Frequency and strain sweeps were performed immediately following under the same conditions. After sample loading, the pH of excess sample volume remaining was measured using a VWR sympHony SB70P pH meter with a Thermo Scientific Orion PerpHecT ROSS Combination pH Micro Electrode. All samples were tested in triplicate (n = 3).

2.5. Scanning Electron Microscopy (SEM)

Hydrogels were fixed in 2% (v/v) glutaraldehyde (Sigma-Aldrich, #G7776) and 3% (m/v) sucrose (J. T. Baker, #4072) in 1× PBS and pH 7.4 for 1 hr at 4 °C. Samples were dehydrated in a graded ethanol series (30-100% in MilliQ H_2O, Decon Laboratories, #2701) of 15 min. intervals and critical-point dried in a Tousimis SAMDRI-790 Critical Point Dryer. For low-magnification SEM, samples were sputter coated with ~10 nm of Au using a Baltec MED-020 Coating System and imaged on a JEOL NeoScope JCM-6000PLUS. For high-magnification SEM, samples were coated with ~9 nm of Os using an SPI Supplies Osmium Plasma Coater OPC-60A and imaged on a Hitachi S-4800 Type II field emission SEM.

2.6. Swelling Analysis

Hydrogel precursor polymer solutions plus PEGX were prepared, and 100 µL of polymer solution was cast into 8-mm diameter cylindrical silicone molds (Grace Bio-Labs). After the 2 hr incubation period, crosslinked hydrogels were carefully removed from molds, and the initial weights ($W_{initial}$) of samples were recorded. Samples were then allowed to equilibrate in 3 mL PBS per sample for 24 hrs at 37 °C. After equilibration, samples were removed from PBS, lightly blotted with filter paper, and weighed. The new equilibrated or swollen wet weights (W_{wet}) of samples were recorded. Samples were then frozen at -80 °C and lyophilized overnight on a VirTis adVantage Plus EL-85, and the dry weights (W_{dry}) of samples were recorded. The percent weight increase and swelling ratio of hydrogels were calculated as follows:

$$\%\ weight\ increase\ = \frac{W_{wet}\ -\ W_{initial}}{W_{initial}} * 100\%$$

$$swelling\ ratio, Q_s = \frac{W_{wet}}{W_{dry}}$$

All samples were weighed on a Mettler Toledo XP105DR Excellence Plus analytical balance, and the sample size was six hydrogels for each group (n = 6).

2.7. Cell Culture

Human umbilical vein endothelial cells (HUVECs) were purchased from Lifeline Cell Technology (normal primary, #FC-0003) and cultured in Endothelial Growth Medium-2 (EGM-2

BulletKit, Lonza, #CC-3162) containing 2% fetal bovine serum (FBS) and growth factors as supplied with the exception of VEGF. Growth factor supplements included: epidermal growth factor, fibroblast growth factor β, R3-insulin-like growth factor-1, ascorbic acid, hydrocortisone, heparin, and gentamicin and amphotericin-B. Cells were cultured at 37 °C in 5% CO_2, media was exchanged every other day, and cells were used between passages 3 and 5 for experimental studies. Conditionally-immortalized human glomerular endothelial cells (GEnCs) were cultured as described previously[29]. These are primary cells that have been transfected with a temperature-sensitive *SV40-T* antigen and the essential catalytic subunit of human telomerase (*hTERT*) to prevent replicative senescence[29, 30]. Culture at the permissive temperature of 33 °C results in active expression of the transgenes to maintain an immature cell state and allow proliferation of the cells. Thermoswitching to the non-permissive temperature of 37 °C results in inactivation of the transgenes, causing the cells to become quiescent and adopt a more mature phenotype that is comparable to freshly isolated GEnCs[29]. GEnCs were cultured in Microvascular Endothelial Growth Medium-2 (EGM-2 MV BulletKit, Lonza, #CC-3202) containing 5% FBS and growth factors as supplied with the exception of VEGF. Growth factor supplements included: epidermal growth factor, fibroblast growth factor β, R3-insulin-like growth factor-1, ascorbic acid, hydrocortisone, and gentamicin and amphotericin-B. Media was exchanged every other day, and cells were used at passage 30 or below for experimental studies.

2.8. Cell Experimental Studies

Experimental studies involving cell culture on hydrogel substrates were performed in a similar manner as previously-established endothelial cell tube formation assays[31, 32]. Hydrogel precursor polymer solutions plus PEGX were prepared and cast in well plates, 165 µL/cm^2, and allowed to incubate for 2 hrs at 37 °C prior to plating of cells. Matrigel Basement Membrane Matrix (Phenol Red-Free, Corning, #356237) served as an additional control for cell experimental studies. Matrigel was thawed on ice, cast in well plates, and incubated alongside experimental groups. Cells were then prepared for plating: cells were rinsed once with 1× Dulbecco's phosphate-buffered saline (DPBS, Mediatech, #21-030), lifted with TrypLE Express (Gibco, #12605) at 37 °C, collected and counted via the trypan blue exclusion method using Trypan Blue solution (Sigma, #T8154), centrifuged, and resuspended in complete media. Cells were plated on substrates at an approximate final density of 48,000 cells/cm^2, and well plates were transferred to a 37 °C incubator at 5% CO_2. At designated time points, photomicrographs of samples were captured on a Lumenera INFINITY*1-3C* microscopy camera mounted on a Nikon Eclipse TS100 using Lumenera INFINITY ANALYZE 6.5 software.

2.9. VEGFR2/KDR Phosphorylation Assay

Phosphorylated VEGFR2 was quantified with the Human Phospho-VEGF R2/KDR DuoSet IC ELISA (R&D Systems, #DYC1766) kit. GEnCs were expanded at 33 °C, plated on culture substrates three days prior to treatment, and cultured at 37 °C after plating. HUVECs were plated on culture substrates two days prior to treatment and cultured at 37 °C. Both HUVECs and GEnCs were fully confluent prior to treatment and sample collection. Cells were serum deprived overnight in Endothelial Basal Medium-2 (EBM-2, Lonza, #CC-3156) plus 1% FBS (Gibco, #16000) and 1% penicillin-streptomycin (Gibco, #15140) prior to treatment and then serum starved in EBM-2 plus 1% penicillin-streptomycin for 5 hrs prior to treatment. Cells were treated with one of the following soluble factors for 5 min. at 37 °C: no treatment (negative control), 100 ng/mL recombinant human VEGF-165 (~5.2 µM, R&D Systems, #293-VE-010/CF) (positive control), 1 µM soluble QK peptide, or no treatment for cells cultured on QK hydrogels (hydrogels conjugated with 100 µM of QK peptide). After treatment, cells were rinsed twice with DPBS and collected with Lysis Buffer #9 composed of Sample Diluent Concentrate 2 (R&D Systems, #DYC002), 10 µg/mL aprotinin (Tocris, #4139), and 10 µg/mL leupeptin (Tocris, #1167) following the kit recommendations. Cell lysates were frozen at -80 °C until assayed following the manufacturer's protocol, and sample

absorbance at 450 nm (A_{450}) corrected by absorbance at 540 nm (A_{540}) was measured on a BioTek Synergy 2 Multi-Mode Microplate Reader. Biological replicates were tested in quadruplicate (n = 4) with technical replicates in duplicate. Samples were compared to a standard curve of Human Phospho-VEGF R2/KDR Control provided by the manufacturer and normalized to negative (no treatment, tissue culture polystyrene substrates) control groups for each cell type.

2.10. Gene Expression Analysis

RNA was isolated from samples and cell pellets using TRIzol Reagent (Invitrogen, #15596) following the manufacturer's protocol. Isolated RNA was treated with DNA-*free* DNA Removal Kit (Ambion, #1906) to remove contaminating genomic DNA from samples. RNA concentration was measured using a NanoDrop 1000 Spectrophotometer (Thermo Scientific). Reverse transcription and cDNA synthesis was performed using iScript Reverse Transcription Supermix for RT-qPCR (Bio-Rad, #170-8841) with an Applied Biosystems GeneAMP PCR System 9700 following the manufacturer's protocol. Real-time quantitative polymerase chain reaction was performed using SsoAdvanced Universal SYBR Green Supermix (Bio-Rad, #170-5270) with an Applied Biosystems QuantStudio 7 Flex Real-Time PCR System. Primer sequences for genes of interest are listed in **Supplemental Table 1**. The thermal profile used included an initial polymerase activation step at 95 °C for 30 sec. followed by 40 amplification cycles of denaturation at 95 °C for 15 sec. and annealing and extension at 60 °C for 60 sec. The expression of each gene of interest was normalized to expression of the housekeeping gene *cyclophilin A* (*PPIA*), and the relative degree of gene amplification was calculated using the $\Delta\Delta C_T$ method: $2^{[(C_T \text{ GOI 2} - C_T \textit{ PPIA } 2) - (C_T \text{ GOI 1} - C_T \textit{ PPIA } 1)]}$. "$C_T$ GOI 1" represents the threshold cycle (C_T) of the gene of interest of the reference population, and "C_T GOI 2" represents the gene of interest of the experimental sample. Day 0 HUVECs cultured on tissue culture polystyrene served as the reference population for HUVEC samples, and day 0 GEnCs cultured on tissue culture polystyrene served as the reference population for GEnC samples. Biological replicates were tested in quadruplicate (n = 4) with technical replicates in triplicate.

2.11. Immunofluorescence

Samples were rinsed once with DPBS and fixed with 4% paraformaldehyde (Alfa Aesar, #43368) in DPBS for 12 min. at room temperature after which fixative was replaced with fresh DPBS, and samples were stored at 4 °C until staining. To perform whole-mount immunofluorescence staining, fixed samples were carefully removed from well plates and transferred to microcentrifuge tubes. Samples were rinsed once with PBS, permeabilized with 0.1% Triton X-100 (Amresco, #0694) in PBS (PBST) for 10 min., and then blocked with Sea Block (Fisher Scientific, #37527) for 30 min. to 1 hr. Primary antibodies were diluted in Sea Block as follows: mouse anti-PECAM-1 at 1:100 (Abcam, #ab187377) and rabbit anti-VEGFR2 at 1:200 (Cell Signaling Technology, #2479). Samples were incubated with primary antibodies for 1 hr at room temperature, rinsed three times with PBST, blocked with Sea Block for an additional 5 min., and then incubated with secondary antibodies for 1 hr at 37 °C. Secondary antibodies were diluted in Sea Block as follows: goat anti-mouse Alexa Fluor 488 at 1:300 (Thermo Fisher, #A11029) and goat anti-rabbit Alexa Fluor 555 at 1:300 (Thermo Fisher, #A21429). After secondary antibody incubation, samples were rinsed three times with PBST, rinsed once with PBS, and mounted between #1.0 glass coverslips (Fisher Scientific, #12-542-B) with Mowiol mounting medium containing 4',6-diamidino-2-phenylindole (DAPI) to stain for cell nuclei. Whole-mount samples were imaged on a Nikon A1 Confocal Laser Microscope System.

2.12. Statistical Analysis

All quantitative data is represented as the mean ± standard error of the mean. Statistical significance was determined using an unpaired two-tailed Student's *t*-test assuming equal

variance with Microsoft Excel (Microsoft). Significance for all statistical analyses was defined as $p < 0.05$.

III. Results

3.1. Optimization of Peptide and PEGX Concentrations

A higher concentration of PEGX was required to adequately conjugate YIGSR peptides to the gelatin polymers at millimolar concentrations and ensure formation of stable hydrogel substrates that would not rapidly degrade in cell culture conditions. Phase analysis of formulations and the resulting phase plot depicts the necessary PEGX concentrations to generate increasingly stiffer hydrogels with conjugated YIGSR concentrations of interest (**Supplemental Figure 1**). Rheological characterization of specific formulations aided in selecting precise PEGX concentrations to generate robust hydrogels of similar stiffness. Hydrogel formulations selected for the following initial cell experiment possessed final storage moduli of ~200-250 Pa.

Hydrogel substrates with varying combinations and concentrations of YIGSR and QK peptides (total of sixteen combinations) were prepared for cell culture to determine optimal peptide concentrations that elicited a discernible cell response. Matrigel was included as an additional group for comparison. GEnCs were plated on hydrogel substrates, and cells were observed in culture over time by optical microscopy. Cells cultured on hydrogels conjugated with 12 mM YIGSR peptide began to form cord-like structures after several hours. After 24 hrs in culture, cells cultured on YIGSR-conjugated hydrogels exhibited cord-like structure formation with branching structures occurring more frequently on hydrogels conjugated with 6 or 12 mM YIGSR peptide (**Supplemental Figure 2**). At the same time, GEnCs also formed smaller yet distinctively apparent cord-like structures on hydrogels conjugated with 10 and 100 µM QK peptide with consistently larger structures forming on hydrogels conjugated with 100 µM QK peptide in comparison to those conjugated with only 10 µM QK peptide (**Supplemental Figure 2**). Therefore, in subsequent investigations, the maximum tested peptide concentrations were chosen, that is 100 µM QK peptide and 12 mM YIGSR peptide (**Table 2**), as these concentrations elicited the greatest and most rapid cell response in this initial experiment.

3.2. Quantification of Free Amine Content

Table 3: Free Amine Content of Hydrogel Precursor Polymer Solutions and Crosslinked Hydrogels

Sample	**No Peptides**	**QK**	**YIGSR**	**YIGSR/QK**
Uncrosslinked				
Normalized Free Amine Content	1.00 ± 0.03	1.03 ± 0.04	1.50 ± 0.03	1.52 ± 0.06
Plus PEGX				
Normalized Free Amine Content	0.77 ± 0.03	0.79 ± 0.09	0.63 ± 0.02	0.70 ± 0.07
% Reacted Amines	23.30 ± 3.06	23.52 ± 8.58	57.84 ± 0.49	54.17 ± 4.94

Quantification of free amine content of hydrogel precursor polymer solutions via the TNBS assay demonstrated that, compared to hydrogel formulations with no peptides, addition of 100 µM QK peptide resulted in only a slight increase of free amine content whereas addition of 12 mM YIGSR peptide resulted in a larger increase of 50% in free amine content (**Table 3** and **Figure 1A**). The addition of the amine-reactive PEGX to crosslink polymer solutions and form hydrogels resulted in a reduction of free amine content for all groups. This reduction corresponded to 20-

25% reacted amines for hydrogels with no peptides and QK hydrogels and 50-60% reacted amines for YIGSR and YIGSR/QK hydrogels (**Table 3** and **Figure 1A**).

3.3. Rheological Characterization and pH Measurements

Table 4: pH and Rheological Characterization of Hydrogels

Sample	No Peptides	QK	YIGSR	YIGSR/QK
pH	6.13 ± 0.01	6.08 ± 0.01	5.87 ± 0.01	5.85 ± 0.01
***G'-G"* Crossover (min)**	10.5 ± 0.60	12.3 ± 0.31	6.5 ± 0.18	4.7 ± 0.24
Storage Modulus, *G'* at 2 hrs (Pa)	198.65 ± 3.57	197.68 ± 15.68	201.02 ± 8.36	214.47 ± 28.89
Loss Modulus, *G"* at 2 hrs (Pa)	1.95 ± 0.05	2.05 ± 0.08	3.00 ± 0.03	2.88 ± 0.09
Complex Shear Modulus, *G* at 2 hrs (Pa)	198.66 ± 3.57	197.69 ± 15.68	201.04 ± 8.36	214.49 ± 28.89

Rheological characterization revealed changes in shear moduli (*G'*, *G"*) during hydrogel formation. Shear moduli measurements are listed in **Table 4** and include the storage modulus (*G'*) and loss modulus (*G"*) crossover point and the storage, loss, and complex shear moduli at 2 hrs. In addition, pH measurement of formulations immediately after addition of PEGX indicate that all formulations fell within a pH range from 5.85 to 6.15 (**Table 4**). Time sweeps demonstrate sigmoidal gelation profiles for all hydrogel formulations (**Figure 1B-E**) with *G'-G"* crossover points between 4.5 and 12.5 min. (**Table 4**) indicating rapid formation of hydrogels after the addition of PEGX. Shear moduli began to stabilize around 1 hr, and final storage and complex shear moduli at 2 hrs for all hydrogels ranged between 195 and 215 Pa (**Table 4**). Frequency sweeps revealed that the *G'* of all hydrogels were relatively independent of the frequencies tested, and the angular frequency value employed for time sweeps was verified to be in the low-frequency plateau region for all formulations (**Supplemental Figure 3A-D**). Strain or amplitude sweeps revealed that the shear moduli of all hydrogels were independent of strain up until 100% strain (the linear viscoelastic region) after which hydrogels exhibited strain-stiffening behavior and catastrophic failure at approximately 1000% strain (**Supplemental Figure 3E-H**).

3.4. Scanning Electron Micrographs and Swelling Analysis of Hydrogels

At low magnifications, scanning electron microscopy revealed relatively flat, homogeneous surfaces for all hydrogels (**Supplemental Figure 4**). At higher magnifications, hydrogels exhibited a porous yet relatively unstructured and amorphous ultrastructure (as opposed to a fibrillar one) (**Figure 2A-D**). Analysis of hydrogels between initial and swollen states demonstrated that hydrogels with no peptides and QK hydrogels exhibited similar percent weight increases of 115.42 ± 4.94 and 120.98 ± 1.49, respectively, whereas YIGSR and YIGSR/QK hydrogels exhibited much greater percent weight increases of 209.30 ± 5.42 and 220.94 ± 2.18, respectively (**Figure 2E**). However, analysis of swelling ratios, that is the ratio of wet to dry weight of samples, revealed that all of the hydrogels exhibited similar swelling ratios between 32 and 35 (**Figure 2F**).

3.5. QK Peptide Bioactivity and Phosphorylation of VEGFR2 in HUVECs and GEnCs

To ensure that the QK peptide was indeed bioactive in the soluble form and that this bioactivity was preserved after conjugation, an ELISA specific to phosphorylated VEGFR2 was used to measure cellular levels of activated and phosphorylated VEGFR2 in response to the QK peptide. Treatment of HUVECs with either soluble $VEGF_{165}$ or soluble QK peptide resulted in significantly increased levels of phosphorylated VEGFR2 relative to untreated controls for HUVECs cultured

on tissue culture polystyrene or on hydrogels with no peptides (**Figure 3A**). HUVECs cultured on QK hydrogels also resulted in significantly increased levels of phosphorylated VEGFR2 relative to HUVECs cultured on hydrogels with no peptides (**Figure 3A**). Surprisingly, treatment of GEnCs with either soluble $VEGF_{165}$ or soluble QK peptide did not result in significant changes in levels of phosphorylated VEGFR2 relative to untreated controls, and this was consistent for both GEnCs cultured on tissue culture polystyrene or on hydrogels with no peptides (**Figure 3B**). In contrast, however, GEnCs cultured on QK hydrogels resulted in significantly increased levels of phosphorylated VEGFR2 relative to GEnCs cultured on hydrogels with no peptides (**Figure 3B**).

3.6. HUVEC Culture, Gene Expression Analysis, and Immunofluorescence

HUVECs were plated on hydrogel substrates and cultured for up to 5 days (**Figure 4**). For cell culture experiments, Matrigel served as positive control because it is commonly utilized in endothelial cell tube formation and angiogenesis assays[31, 32]. RYGSI hydrogels served as an additional scrambled YIGSR peptide control to account for the increased concentration of PEGX necessary in YIGSR and YIGSR/QK hydrogel formulations. On Matrigel, HUVECs underwent rapid morphogenesis and formed an interconnected network within 6 hrs that began to regress by 24 hrs and was completely absent after 3 days though cell aggregates could be observed at the sides of wells. On hydrogels with no peptides, HUVECs proliferated to form a monolayer approximately 60-70% confluent by 24 hrs, and cells continued to proliferate resulting in the cord-like structures observed at day 3 and beyond. On QK hydrogels, a similar response was observed as HUVECs cultured on hydrogels with no peptides. On YIGSR hydrogels, HUVECs began to form cord-like structures by 6 hrs that increased in size and connections by 24 hrs, but cells did not form a confluent monolayer by day 5, and instead the network formed by the cord-like structures appeared to tighten. On YIGSR/QK hydrogels, a similar response was observed as HUVECs cultured on YIGSR hydrogels. On RYGSI hydrogels, HUVECs began to form cord-like structures by 6 hrs in a similar manner as on YIGSR and YIGSR/QK hydrogels; however, cells continued to proliferate and formed a confluent monolayer by day 3 with cord-like structures still present.

Genes of interest included in gene expression analysis are involved in cell-cell interactions (*PECAM1*, *CDH5*/VE-Cad), cell-matrix interactions via integrins (*ITGB1*, *ITGB3*), signaling pathways via cell surface receptors (*KDR*/VEGFR2, *TEK*/TIE2), and endothelial function (*VWF*, *NOS3*, *PLVAP*) (**Figure 5**). In general, gene expression analysis revealed highest fold-change expression by HUVECs cultured on YIGSR/QK hydrogels at day 5 (**Figure 5A-I**). This is true for *CDH5* (**Figure 5B**), *ITGB3* (**Figure 5D**), *KDR* (**Figure 5E**), *TEK* (**Figure 5F**), *VWF* (**Figure 5G**), and *NOS3* (**Figure 5H**). For *PECAM1* (**Figure 5A**) and *ITGB1* (**Figure 5C**), HUVECs exhibited greatest upregulation on QK hydrogels at 24 hrs, and for *PLVAP* (**Figure 5I**), HUVECs exhibited greatest upregulation on Matrigel at 24 hrs. HUVECs cultured on RYGSI hydrogels generally exhibited the lowest fold-change expression of genes compared to other groups at all time points. Immunofluorescence staining confirmed the expression of platelet endothelial cell adhesion molecule (PECAM-1 or CD31 encoded by *PECAM1*) and of VEGFR2 (encoded by *KDR*) by HUVECs cultured on no peptide, QK, YIGSR, and YIGSR/QK hydrogels at 6 and 24 hrs (**Figure 5J**).

3.7. GEnC Culture and Gene Expression Analysis

GEnCs were similarly plated on hydrogel substrates and cultured for up to 5 days at the non-permissive temperature (**Figure 6**). On Matrigel, GEnCs underwent rapid morphogenesis and formed an interconnected network within 6 hrs that rapidly regressed by 24 hrs, and by 3 days only large cell aggregates remained. On hydrogels with no peptides, GEnCs proliferated slowly

as the transgenes began to degrade resulting in a fully confluent and stable monolayer on days 3 and 5. On QK hydrogels, GEnCs proliferated in a similar manner as on hydrogels with no peptides; however, this proliferation resulted in the formation of cord-like structures not seen on hydrogels with no peptides at day 5. On YIGSR hydrogels, GEnCs began to form cord-like structures by 6 hrs that continued to form connections over the culture period; however, the cells did not form a confluent monolayer by day 5 and appear morphologically distinct compared to the cord-like structures formed by HUVECs on the same hydrogels (**Figure 4**). On YIGSR/QK hydrogels, a similar response was observed as GEnCs cultured on YIGSR hydrogels. On RYGSI hydrogels, GEnCs began to form cord-like structures by 6 hrs in a similar manner as on YIGSR and YIGSR/QK hydrogels; however, cells were not homogeneously distributed across the hydrogel and instead clustered towards the center of the well, which resulted in the formation of a confluent monolayer in the center of the well by day 5 and cord-like structures that present as denser in appearance.

Gene expression analysis results of GEnC cultures were generally more varied than results from HUVEC cultures, and fold-change expression by GEnCs was generally lower than HUVECs (**Figure 7**). GEnCs exhibited greatest fold-change expression on Matrigel at day 5 for *PECAM1* (**Figure 7A**), *CDH5* (**Figure 7B**), *KDR* (**Figure 7E**), *TEK* (**Figure 7F**), *VWF* (**Figure 7G**), and *PLVAP* (**Figure 7I**). In addition, GEnCs cultured on RYGSI hydrogels exhibited high fold-change expression of genes such as *PECAM1*, *CDH5*, and *ITGB3* (**Figure 7D**) at day 5 and *ITGB1* (**Figure 7C**) and *TEK* at 6 hrs.

IV. Discussion

The BM, a structure composed of layered ECM molecules, underlies epithelial and endothelial cell populations and provides a dynamic interface between these cells and the surrounding parenchyma[5]. Recapitulating the unique properties of the BM using synthetic biomaterial systems, such as hydrogel matrices, requires careful modulation of the system's physicochemical properties[6]. In this work, we employed a versatile chemical crosslinking strategy, the PEGX method, to generate stable gelatin hydrogels for cell culture while simultaneously conjugating synthetic peptides to the gelatin polymer backbone to impart additional bioactivity. The two peptides of interest for these investigations were the laminin-derived YIGSR peptide[11, 12] and the VEGF-mimetic QK peptide[19]. Material characterization of the hydrogel formulations included rheological, ultrastructural, and swelling analyses, and *in vitro* studies with HUVECs and GEnCs were performed to evaluate performance of the hydrogels as a BM mimic for endothelial cell culture.

Hydrogels are highly hydrated, crosslinked networks of polymers. In the current investigation, the formation of a hydrogel from a precursor polymer solution occurs when the PEGX SVA functional groups react with free amines present on the gelatin polymers resulting in a covalently-crosslinked gelatin network (**Scheme 1**). Using this system, hydrogels can be additionally functionalized with bioactive molecules containing free amine groups such as synthetic peptides. Quantification of the free amine content of hydrogel precursor polymer solutions and crosslinked hydrogels via the TNBS assay confirmed that crosslinking occurs as a result of the PEGX reacting with free amine groups (**Figure 1A**). As expected, the percentage of reacted amines for the hydrogels with no peptides (**Table 3**) was similar in range to results presented in a previously published investigation demonstrating the utility the PEGX method[7]. Furthermore, the addition of the YIGSR peptide at a concentration of 12 mM increased the free amine content of the respective hydrogel precursor polymer solutions to approximately 1.5 times that of polymer solutions with no peptides, and addition of PEGX resulted in normalized free amine content values below that of crosslinked hydrogels with no peptides. This indicates that both successful crosslinking between

gelatin polymers as well as conjugation of the YIGSR peptide to the gelatin polymer network occurred. It is possible that other products will result from the crosslinking reaction, such as the reaction of a single PEGX molecule with two peptides; however, we expect these products to occur at a much lower frequency than the desired conjugation of peptides to the gelatin polymers due to the greater availability of free amines on the gelatin.

Successful crosslinking of the hydrogel precursor polymer solutions was further confirmed by rheological characterization. Time sweeps and shear moduli measurements revealed rapid crosslinking of formulations and *G'-G"* crossovers (that is, the time at which the elastic or solid-like properties matched the viscous or liquid-like properties of the sample) within several minutes after the addition of PEGX (**Table 4**). Shear moduli were mostly stable by 2 hrs, indicating the crosslinking reaction was nearly complete by this time (**Figure 1B-E**). Final storage and complex shear moduli of hydrogels were of similar magnitudes and within the range of 195 to 215 Pa (**Table 4**).

This narrow range of storage moduli was intended to eliminate hydrogel stiffness as a possible confounding factor that could influence cellular response. It has been well-documented that cells respond to the mechanical properties of their microenvironment through mechanotransduction[33, 34]. Substrate stiffness will not only influence endothelial cell morphology and actin stress fiber formation[35, 36] but also modulate expression of growth factors and receptor proteins[37]. Ultimately, these factors influence endothelial morphogenesis and capillary network formation[35, 38-40]. In these investigations, storage moduli of approximately 200 Pa were desired as the BM-like archetype Matrigel control has a reported storage modulus of 55 to 90 Pa[28, 41]; however, "soft" hydrogel formulations crosslinked via the PEGX method (those with storage moduli below 150 Pa) previously were shown to degrade rapidly in cell culture conditions[7], so a balance between substrate stiffness and rate of degradation was necessary.

Additional frequency and strain sweeps confirmed the formation of elastic hydrogels after crosslinking (**Supplemental Figure 3**). Interestingly, the hydrogels exhibited strain stiffening when exposed to strains between 100% and 1000%. Strain stiffening is a common behavior among biological materials, such as fibrin, type I collagen, and kidney decellularized extracellular matrix hydrogels, but is typically difficult to recapitulate with synthetic polymer networks[42-44]. Although these hydrogels are formed through covalent crosslinks using a synthetic crosslinker, the strain-stiffening behavior suggests that interactions between the gelatin polymers such as physical associations may still influence the resulting network structure.

Ultrastructural analysis of hydrogel surfaces via SEM did not demonstrate any considerable variation across groups (**Figure 2A-D**). Swelling analysis of hydrogels, however, revealed a distinction between hydrogels without conjugated YIGSR peptide and YIGSR-conjugated hydrogels. Investigating the percent weight increase between initial and swollen hydrogel states, we found that YIGSR and YIGSR/QK hydrogels tripled in weight (~200% increase) whereas hydrogels with no peptides and QK hydrogels only doubled in weight (~100% increase) (**Figure 2E**). However, the swelling ratios between swollen hydrogel and dry polymer states was relatively similar across groups (**Figure 2F**). This indicates that this distinction was a result of the increased dry polymer weight of YIGSR-conjugated hydrogels, which not only have the addition of the YIGSR peptide but also higher concentrations of PEGX (**Table 2**). To account for this additional variable, a scrambled YIGSR peptide control (the RYGSI peptide) previously shown to lack the cell-binding activity of the YIGSR peptide[16] was included in later cell studies.

The VEGF-mimetic QK peptide has been reported to bind VEGF receptors resulting in activation of downstream intracellular signaling pathways in endothelial cells, and in particular

pathways downstream of VEGFR2[19, 45]. Activation of VEGFR2 leads to dimerization of receptors and autophosphorylation of intracellular tyrosine residues[46]. After activation, VEGFR2 is internalized during which signaling continues until the receptor is degraded or undergoes desphosphorylation and recycling[47]. Importantly, studies suggest that internalization of VEGF itself is not necessary for phosphorylation of VEGFR2 and downstream signaling[48]. Therefore, utilizing a commercially-available intracellular ELISA kit, we demonstrated that soluble QK peptide indeed resulted in significantly elevated levels of phosphorylated VEGFR2 in HUVECs, and this activity was preserved even after conjugation to crosslinked gelatin hydrogel substrates using PEGX (**Figure 3A**).

Surprisingly, this activity did not appear to be consistent between cell types as treatment with soluble QK peptide did not result in significant changes in levels of phosphorylated VEGFR2 in GEnCs (**Figure 3B**). In addition, although the treatment of HUVECs with soluble $VEGF_{165}$ resulted in significantly elevated levels of phosphorylated VEGFR2 as expected, this was not the case for GEnCs treated for the same duration and with the same concentration of $VEGF_{165}$. In contrast, GEnCs cultured on QK hydrogels exhibited significantly elevated levels of phosphorylated VEGFR2. This is particularly intriguing as matrix-bound VEGF has been found to preferentially activate VEGFR2 signaling pathways involved in cell migration[49] and result in endothelial vessels that are smaller in diameter and contain more branching points in a tumor model[50]. As a specialized microvascular endothelial cell population, it is possible that the GEnCs are more responsive to matrix-bound VEGF (or in this case, matrix-bound QK peptide) as this would result in endothelial structures more reminiscent of microvascular beds. This is further supported by knowledge that heparan sulfate proteoglycans within the glomerular basement membrane[51] may sequester growth factors with heparin-binding domains, including $VEGF_{165}$[52, 53]. $VEGF_{165}$ is the predominant VEGF isoform secreted by podocytes[54], the specialized perivascular cells that form the external layer of the glomerular filtration barrier, and this VEGF secretion by podocytes is crucial in the formation and maintenance of the glomerular filtration barrier[53, 55]. Therefore, these results may help tie together the unique physical path and regulation of VEGF within the glomerulus: from secretion by podocytes, to sequestration within the glomerular basement membrane, and finally presentation to GEnCs.

HUVECs were employed as readily-available and prototypical cells for investigating endothelial cell response to culture on our hydrogel substrates (**Figure 4**). HUVECs cultured on Matrigel rapidly assembled into multicellular, tube-like networks that later regressed into cell aggregates, as expected[31, 32]. While HUVECs cultured on hydrogels with no peptides and QK hydrogels formed confluent monolayers, HUVECs cultured on YIGSR and YIGSR/QK hydrogels formed cord-like structures that persisted throughout the culture period. To our surprise, however, HUVECs cultured on RYGSI hydrogel responded in a similar manner forming cord-like structures. This suggests that the cord-like structure formation observed was not a result of the bioactivity of the YIGSR peptide but instead due to some other factor. Swelling analysis, discussed previously, revealed that YIGSR-conjugated hydrogels exhibited greater percent weight increases relative to hydrogels with no peptides and QK hydrogels, which is likely an effect of the increased dry polymer content of these formulations (**Figure 2E-F** and **Table 2**). Therefore, when confined to the well dimensions in a cell culture plate, YIGSR-conjugated and similarly RYGSI hydrogels swell to a greater extent than hydrogels with no peptides and QK hydrogels, resulting in an uneven culture surface or regions of tension and compression that may influence local cellular adhesion and migration.

Gene expression analysis of cultures, however, demonstrated that the addition of conjugated bioactive peptides led to changes in expression of many genes of interest in HUVECs (**Figure 5**). In several instances, these changes were upregulated in comparison to culture on hydrogels with

no peptides, and ultimately the combined synergistic effects of the peptides in YIGSR/QK hydrogels resulted in the highest fold-change expression by day 5. On the other hand, although HUVECs formed similar cord-like structures on RYGSI hydrogels, gene expression analysis demonstrated that conjugation of the inactive peptide resulted in downregulation of most of the genes of interest. This downregulation was often even below expression levels of cells cultured on hydrogels with no peptides, which is likely an effect of the increased PEG content of RYGSI hydrogels that would alter both the density of available cell-binding sites as well as the swelling properties and thus surface topography of the hydrogel substrates.

Conditionally-immortalized human GEnCs were also employed as an additional cell type for investigating endothelial cell response to culture on our hydrogel substrates (**Figure 6**). GEnCs cultured on hydrogels with no peptides formed confluent monolayers, and addition of conjugated QK peptide resulted in some cord-like structure formation by cells. While GEnCs cultured on YIGSR and YIGSR/QK hydrogels also seemed to form cord-like structures, these structures appeared less dense than those formed by HUVECs on the same hydrogel substrates. Interestingly, structures formed on RYGSI hydrogels by GEnCs and HUVECs appear more similar to each other, which again suggests that the bioactivity of the YIGSR peptide plays an important role in modulating cell response.

Gene expression analysis of cultures likewise demonstrated quite different trends between GEnCs and HUVECs (**Figure 7**). For many genes of interest, the conjugation of bioactive peptides did not lead to significant changes in gene expression. Instead, GEnCs exhibited the highest fold-change expression on Matrigel and RYGSI hydrogels, typically at day 5. Correlating these results with images of the cultures, GEnCs seem to prefer extensive cell-cell interactions that form during cell aggregation over cell-matrix interactions. This corresponded to upregulation of genes involved in cell-cell interactions such as *PECAM1* and *CDH5*, cell surface receptors involved in signaling pathways such as *KDR* and *TEK*, and endothelial function such as *VWF* and *PVLAP*. These results reinforce findings from a previous investigation in which GEnCs encapsulated within kidney decellularized extracellular matrix hydrogels exhibited lower fold-change expression of many of the same genes of interest in comparison to cells encapsulated within type I collagen hydrogels in part due to an inability to form strong cell-cell interactions[44].

The differences in cell response by HUVECs and GEnCs is ultimately not unexpected. Endothelial vessels and vascular beds in the body are phenotypically heterogeneous and occupy a diverse range of physiological microenvironments[56, 57]. It is not surprising that when isolated from an *in vivo* setting and cultured *in vitro*, these various cell populations will respond differently. For example, Ligresti, *et al*. isolated human kidney peritubular microvascular endothelial cells (HKMECs) and through functional and molecular assays found that these cells lack intrinsic regenerative growth capacity and angiogenic potential, which is in contrast to the proliferative nature of HUVECs[58]. Further investigations by the same group additionally highlighted the distinct responses HKMECs exhibited in comparison to HUVECs when cells were cultured on hydrogel substrates composed of type I collagen, kidney cortex decellularized extracellular matrix, or a combination of both materials[59]. Similar to these HKMECs, GEnCs are a specialized microvascular endothelial cell population isolated from a specific region of the kidney. Therefore, it follows that the GEnCs will invariably respond in a much different manner in comparison to HUVECs as we have seen from our results.

Altogether, we have demonstrated the use of the PEGX method to generate stable, crosslinked gelatin hydrogels suitable for cell culture. Furthermore, this versatile crosslinking method permits the additional conjugation of bioactive peptides to the polymer backbone as a strategy to modulate cell response. Several groups have previously demonstrated a variety of

methods for generating peptide-modified PEG hydrogels or PEG-peptide composite hydrogels, including mixed mode thiol-acrylate photopolymerization using PEG diacrylate[60], PEG-peptide macromers for subsequent photopolymerization using PEG acrylate[61] or PEG diacrylate[62], thiol-ene photocoupling using PEG-norbornene[63, 64], and self-assembled peptide amphiphile and photopolymerizable PEG dimethacrylate composite hydrogels[65]. However, in comparison, the synthetic-natural PEG-gelatin composite hydrogels investigated here promote cell adhesion and permit cell-mediated degradation even in the absence of additional peptides. This again demonstrates the versatility of the PEGX method as demonstrated here and elsewhere[7].

Furthermore, unlike the above referenced investigations, the PEGX chemistry utilized in this work does not require a photo-mediated reaction and thus eliminates the need for a photoinitiator. However, using the specific single SVA-PEG-SVA crosslinker explored in this study, polymer crosslinking and conjugation of additional bioactive molecules necessitates increasing the total polymer weight of formulations depending on the concentrations of the molecules of interest. This can lead to confounding variables such as changes in hydrogel swelling and cell-binding ligand densities. Future investigations may opt to explore PEGX physical and chemical variants, such as multi-arm PEG crosslinkers[7] or bioorthogonal “click” chemistries[66, 67], to crosslink polymers and conjugate multiple bioactive molecules using orthogonal reactions for greater control of hydrogel properties. Ultimately, advances in engineering BM-like hydrogel substrates will not only enhance physiological understanding of cell-cell and cell-matrix interactions but also accelerate the development of tissue models for drug testing and novel strategies for regenerative therapies.

V. Conclusion

The PEGX method is a versatile crosslinking strategy that, in this study, was used to simultaneously generate stable, crosslinked gelatin hydrogels as well as conjugate bioactive peptides onto the gelatin polymers. Hydrogels formed from precursor polymer solutions within several minutes after the addition of PEGX, but differential swelling properties occurred as a result of adjusting peptide and PEGX concentrations. These peptide-conjugated hydrogels were investigated as cell culture substrates for two human endothelial cell types, human umbilical vein endothelial cells and human glomerular endothelial cells, that exhibited uniquely different cell behavior evaluated by measuring levels of phosphorylated VEGFR2 and changes in gene expression. Future investigations may explore additional PEGX variants for crosslinking and conjugation reactions, a variety of polymers or bioactive molecules for biofunctionalization, or other cells types to evaluate cellular response. Ultimately, these studies contribute to the growing interest in developing basement membrane-like hydrogels for delineating complex epithelial and endothelial cell-cell and cell-matrix interactions.

VI. Supplementary Material

Supplementary materials are available online at: [LINK]

VII. Acknowledgements

The authors would like to acknowledge the use of the following research facilities: the Analytical bioNanoTechnology Equipment Core Facility (ANTEC) of the Simpson Querrey Institute (SQI) at Northwestern University developed by support from the U.S. Army Research Office, the U.S. Army Medical Research and Materiel Command, and Northwestern University with ongoing support from the Soft and Hybrid Nanotechnology Experimental (SHyNE) Resource (NSF ECCS-1542205); the Electron Probe Instrumentation Center (EPIC) of Northwestern University’s Atomic and Nanoscale Characterization Experimental Center (NU*ANCE*), which has

received support from the Soft and Hybrid Nanotechnology Experimental (SHyNE) Resource (NSF ECCS-1542205), the Materials Research Science and Engineering Centers (MRSECs) program (NSF DMR-1720139) at the Materials Research Center (MRC), the International Institute for Nanotechnology (IIN), the Keck Foundation, and the State of Illinois through the IIN; the Northwestern University Center for Advanced Microscopy (CAM) supported by NCI CCSG P30 CA060553 awarded to the Robert H. Lurie Comprehensive Cancer Center; the NUSeq Core Facility supported by the Northwestern University Center for Genetic Medicine, Feinberg School of Medicine, and Shared and Core Facilities of the University's Office for Research; and the George M. O'Brien Kidney Research Core Center (NU GoKidney) supported by NIDDK P30DK114857.

VIII. Author Contributions & Funding Sources

J.S.: Designed and performed experiments, optimized testing parameters, collected and analyzed data, and wrote and edited the manuscript including figures. S.C.S: Provided the conditionally-immortalized human glomerular endothelial cell line and contributed to experimental design. J.A.W.: Co-principal investigator who assisted with experimental design, interpretation of data, and manuscript writing and editing. R.N.S.: Co-principal investigator who assisted with experimental design, interpretation of data, and manuscript writing and editing. All authors read and approved the manuscript. This work was supported by a National Institutes of Health Ruth L. Kirschstein National Research Service Award (NRSA) Individual Predoctoral Fellowship (NIDDK F31 DK108544) awarded to J.S. This research was supported by grants from the Google Foundation (R.N.S.) and the McCormick Foundation (J.A.W.). This research was also supported in part by NIDDK R01 DK113168 from the National Institutes of Health (J.A.W.) and Merit Review I01 BX002660 from the United States Department of Veterans Affairs Biomedical Laboratory Research and Development Service (J.A.W). J.A.W. is a member of the NIDDK (Re)Building a Kidney Consortium (U01 DK107350). The contents presented do not represent the views of the United States Department of Veterans Affairs, the National Institutes of Health, or the United States Government. Funding sources had no involvement in study design; collection, analysis, or interpretation of data; in writing of the manuscript; or in the decision to submit the manuscript for publication.

IX. Disclosures

R.N.S. declares financial interests in Dimension Inx, LLC, which may potentially benefit from the outcomes of this research. All other authors declare that they have no conflicts of interest.

X. References

[1] Frantz C, Stewart KM, and Weaver VMJJCS. "The extracellular matrix at a glance." *Journal of cell science* **123** (2010): 4195-4200.

[2] Badylak SF, Freytes DO, and Gilbert TW. "Extracellular matrix as a biological scaffold material: Structure and function." *Acta Biomaterialia* **5** (2009): 1-13.

[3] Tibbitt MW, and Anseth KS. "Hydrogels as extracellular matrix mimics for 3d cell culture." *Biotechnology and bioengineering* **103** (2009): 655-663.

[4] Geckil H, Xu F, Zhang X, Moon S, and Demirci U. "Engineering hydrogels as extracellular matrix mimics." *Nanomedicine* **5** (2010): 469-484.

[5] Yurchenco PD. "Basement membranes: Cell scaffoldings and signaling platforms." *Cold Spring Harbor Perspectives in Biology* **3** (2011): a004911.

[6] Cruz-Acuña R, and García AJ. "Synthetic hydrogels mimicking basement membrane matrices to promote cell-matrix interactions." *Matrix Biology* **57** (2017): 324-333.

[7] Rutz AL, Hyland KE, Jakus AE, Burghardt WR, and Shah RN. "A multimaterial bioink method for 3d printing tunable, cell-compatible hydrogels." *Advanced Materials* **27** (2015): 1607-1614.

[8] Tabata Y, and Ikada Y. "Protein release from gelatin matrices." *Advanced drug delivery reviews* **31** (1998): 287-301.

[9] Van Vlierberghe S, Dubruel P, and Schacht E. "Biopolymer-based hydrogels as scaffolds for tissue engineering applications: A review." *Biomacromolecules* **12** (2011): 1387-1408.

[10] Rutz AL, and Shah RN. "Protein-based hydrogels." *Polymeric hydrogels as smart biomaterials.* Springer: (2016).

[11] Graf J, Iwamoto Y, Sasaki M, Martin GR, Kleinman HK, Robey FA, and Yamada Y. "Identification of an amino acid sequence in laminin mediating cell attachment, chemotaxis, and receptor binding." *Cell* **48** (1987): 989-996.

[12] Graf J, Ogle RC, Robey FA, Sasaki M, Martin GR, Yamada Y, and Kleinman HK. "A pentapeptide from the laminin b1 chain mediates cell adhesion and binds to 67000 laminin receptor." *Biochemistry* **26** (1987): 6896-6900.

[13] Jun H-W, and West J. "Development of a yigsr-peptide-modified polyurethaneurea to enhance endothelialization." *Journal of Biomaterials Science, Polymer Edition* **15** (2004): 73-94.

[14] Jun HW, and West JL. "Modification of polyurethaneurea with peg and yigsr peptide to enhance endothelialization without platelet adhesion." *Journal of Biomedical Materials Research Part B: Applied Biomaterials* **72** (2005): 131-139.

[15] Jun H-W, and West JL. "Endothelialization of microporous yigsr/peg-modified polyurethaneurea." *Tissue engineering* **11** (2005): 1133-1140.

[16] Jung JP, Moyano JV, and Collier JH. "Multifactorial optimization of endothelial cell growth using modular synthetic extracellular matrices." *Integrative Biology* **3** (2011): 185-196.

[17] Fittkau M, Zilla P, Bezuidenhout D, Lutolf M, Human P, Hubbell JA, and Davies N. "The selective modulation of endothelial cell mobility on rgd peptide containing surfaces by yigsr peptides." *Biomaterials* **26** (2005): 167-174.

[18] Ali S, Saik JE, Gould DJ, Dickinson ME, and West JL. "Immobilization of cell-adhesive laminin peptides in degradable pegda hydrogels influences endothelial cell tubulogenesis." *BioResearch open access* **2** (2013): 241-249.

[19] D'Andrea LD, Iaccarino G, Fattorusso R, Sorriento D, Carannante C, Capasso D, Trimarco B, and Pedone C. "Targeting angiogenesis: Structural characterization and biological properties of a de novo engineered vegf mimicking peptide." *Proceedings of the national academy of sciences of the United States of America* **102** (2005): 14215-14220.

[20] Olsson A-K, Dimberg A, Kreuger J, and Claesson-Welsh L. "Vegf receptor signalling? In control of vascular function." *Nature reviews Molecular cell biology* **7** (2006): 359-371.

[21] Vlieghe P, Lisowski V, Martinez J, and Khrestchatisky M. "Synthetic therapeutic peptides: Science and market." *Drug discovery today* **15** (2010): 40-56.
[22] Cai L, Dinh CB, and Heilshorn SC. "One-pot synthesis of elastin-like polypeptide hydrogels with grafted vegf-mimetic peptides." *Biomaterials science* **2** (2014): 757-765.
[23] Chan TR, Stahl PJ, and Yu SM. "Matrix-bound vegf mimetic peptides: Design and endothelial-cell activation in collagen scaffolds." *Advanced Functional Materials* **21** (2011): 4252-4262.
[24] Leslie-Barbick JE, Saik JE, Gould DJ, Dickinson ME, and West JL. "The promotion of microvasculature formation in poly (ethylene glycol) diacrylate hydrogels by an immobilized vegf-mimetic peptide." *Biomaterials* **32** (2011): 5782-5789.
[25] Parthiban SP, Rana D, Jabbari E, Benkirane-Jessel N, and Ramalingam M. "Covalently immobilized vegf-mimicking peptide with gelatin methacrylate enhances microvascularization of endothelial cells." *Acta Biomaterialia* **51** (2017): 330-340.
[26] Habeeb ASA. "Determination of free amino groups in proteins by trinitrobenzenesulfonic acid." *Analytical biochemistry* **14** (1966): 328-336.
[27] Kuijpers AJ, Engbers GH, Krijgsveld J, Zaat SA, Dankert J, and Feijen J. "Cross-linking and characterisation of gelatin matrices for biomedical applications." *Journal of Biomaterials Science, Polymer Edition* **11** (2000): 225-243.
[28] Zuidema JM, Rivet CJ, Gilbert RJ, and Morrison FA. "A protocol for rheological characterization of hydrogels for tissue engineering strategies." *Journal of Biomedical Materials Research Part B: Applied Biomaterials* **102** (2014): 1063-1073.
[29] Satchell SC, Tasman CH, Singh A, Ni L, Geelen J, von Ruhland CJ, O'Hare MJ, Saleem MA, van den Heuvel LP, and Mathieson PW. "Conditionally immortalized human glomerular endothelial cells expressing fenestrations in response to vegf." *International Society of Nephrology* **69** (2006): 1633-1640.
[30] Ali SH, and DeCaprio JA. "Cellular transformation by sv40 large t antigen: Interaction with host proteins." *Seminars in Cancer Biology* **11** (2001): 15-22.
[31] Arnaoutova I, George J, Kleinman HK, and Benton G. "The endothelial cell tube formation assay on basement membrane turns 20: State of the science and the art." *Angiogenesis* **12** (2009): 267-274.
[32] Arnaoutova I, and Kleinman HK. "In vitro angiogenesis: Endothelial cell tube formation on gelled basement membrane extract." *Nature protocols* **5** (2010): 628-635.
[33] Discher DE, Janmey P, and Wang Y-l. "Tissue cells feel and respond to the stiffness of their substrate." *Science* **310** (2005): 1139-1143.
[34] Levental I, Georges PC, and Janmey PA. "Soft biological materials and their impact on cell function." *Soft Matter* **3** (2007): 299-306.
[35] Sieminski A, Hebbel R, and Gooch K. "The relative magnitudes of endothelial force generation and matrix stiffness modulate capillary morphogenesis in vitro." *Experimental Cell Research* **297** (2004): 574-584.
[36] Byfield FJ, Reen RK, Shentu T-P, Levitan I, and Gooch KJ. "Endothelial actin and cell stiffness is modulated by substrate stiffness in 2d and 3d." *Journal of biomechanics* **42** (2009): 1114-1119.
[37] Santos L, Fuhrmann G, Juenet M, Amdursky N, Horejs CM, Campagnolo P, and Stevens MM. "Extracellular stiffness modulates the expression of functional proteins and growth factors in endothelial cells." *Advanced healthcare materials* **4** (2015): 2056-2063.
[38] Davis GE, and Camarillo CW. "Regulation of endothelial cell morphogenesis by integrins, mechanical forces, and matrix guidance pathways." *Experimental Cell Research* **216** (1995): 113-123.
[39] Califano JP, and Reinhart-King CA. "A balance of substrate mechanics and matrix chemistry regulates endothelial cell network assembly." *Cellular and molecular bioengineering* **1** (2008): 122.

[40] Sun J, Jamilpour N, Wang F-Y, and Wong PK. "Geometric control of capillary architecture via cell-matrix mechanical interactions." *Biomaterials* **35** (2014): 3273-3280.
[41] Zaman MH, Trapani LM, Sieminski AL, MacKellar D, Gong H, Kamm RD, Wells A, Lauffenburger DA, and Matsudaira P. "Migration of tumor cells in 3d matrices is governed by matrix stiffness along with cell-matrix adhesion and proteolysis." *Proceedings of the National Academy of Sciences* **103** (2006): 10889-10894.
[42] Storm C, Pastore JJ, MacKintosh FC, Lubensky TC, and Janmey PA. "Nonlinear elasticity in biological gels." *Nature* **435** (2005): 191-194.
[43] Erk KA, Henderson KJ, and Shull KR. "Strain stiffening in synthetic and biopolymer networks." *Biomacromolecules* **11** (2010): 1358-1363.
[44] Su J, Satchell SC, Shah RN, and Wertheim JA. "Kidney decellularized extracellular matrix hydrogels: Rheological characterization and human glomerular endothelial cell response to encapsulation." *Journal of Biomedical Materials Research Part A* **106A** (2018): 2448-2462.
[45] Finetti F, Basile A, Capasso D, Di Gaetano S, Di Stasi R, Pascale M, Turco CM, Ziche M, Morbidelli L, and D'Andrea LD. "Functional and pharmacological characterization of a vegf mimetic peptide on reparative angiogenesis." *Biochemical pharmacology* **84** (2012): 303-311.
[46] Holmes K, Roberts OL, Thomas AM, and Cross MJ. "Vascular endothelial growth factor receptor-2: Structure, function, intracellular signalling and therapeutic inhibition." *Cellular signalling* **19** (2007): 2003-2012.
[47] Koch S, Tugues S, Li X, Gualandi L, and Claesson-Welsh L. "Signal transduction by vascular endothelial growth factor receptors." *Biochemical journal* **437** (2011): 169-183.
[48] Anderson SM, Shergill B, Barry ZT, Manousiouthakis E, Chen TT, Botvinick E, Platt MO, Iruela-Arispe ML, and Segura T. "Vegf internalization is not required for vegfr-2 phosphorylation in bioengineered surfaces with covalently linked vegf." *Integrative Biology* **3** (2011): 887-896.
[49] Chen TT, Luque A, Lee S, Anderson SM, Segura T, and Iruela-Arispe ML. "Anchorage of vegf to the extracellular matrix conveys differential signaling responses to endothelial cells." *The Journal of cell biology* **188** (2010): 595-609.
[50] Lee S, Jilani SM, Nikolova GV, Carpizo D, and Iruela-Arispe ML. "Processing of vegf-a by matrix metalloproteinases regulates bioavailability and vascular patterning in tumors." *The Journal of cell biology* **169** (2005): 681-691.
[51] Miner JH. "The glomerular basement membrane." *Experimental Cell Research* **318** (2012): 973-978.
[52] Ferrara N. "Vascular endothelial growth factor: Basic science and clinical progress." *Endocrine reviews* **25** (2004): 581-611.
[53] Eremina V, Baelde HJ, and Quaggin SE. "Role of the vegf-a signaling pathway in the glomerulus: Evidence for crosstalk between components of the glomerular filtration barrier." *Nephron Physiology* **206** (2007): 32-37.
[54] Kretzler M, Schröppel B, Merkle M, Huber S, Mundel P, Horster M, and Schlöndorff D. "Detection of multiple vascular endothelial growth factor splice isoforms in single glomerular podocytes." *Kidney International* **54** (1998): S159-S161.
[55] Scott RP, and Quaggin SE. "The cell biology of renal filtration." *The Journal of cell biology* **209** (2015): 199-210.
[56] Aird WC. "Phenotypic heterogeneity of the endothelium: I. Structure, function, and mechanisms." *Circulation research* **100** (2007): 158-173.
[57] Aird WC. "Phenotypic heterogeneity of the endothelium: Ii. Representative vascular beds." *Circulation research* **100** (2007): 174-190.

[58] Ligresti G, Nagao RJ, Xue J, Choi YJ, Xu J, Ren S, Aburatani T, Anderson SK, MacDonald JW, and Bammler TK. "A novel three–dimensional human peritubular microvascular system." *Journal of the American Society of Nephrology* **27** (2016): 2370-2381.

[59] Nagao RJ, Xu J, Luo P, Xue J, Wang Y, Kotha S, Zeng W, Fu X, Himmelfarb J, and Zheng Y. "Decellularized human kidney cortex hydrogels enhance kidney microvascular endothelial cell maturation and quiescence." *Tissue Engineering Part A* **22** (2016): 1140-1150.

[60] Salinas CN, and Anseth KS. "Mixed mode thiol− acrylate photopolymerizations for the synthesis of peg− peptide hydrogels." *Macromolecules* **41** (2008): 6019-6026.

[61] Moon JJ, Saik JE, Poche RA, Leslie-Barbick JE, Lee S-H, Smith AA, Dickinson ME, and West JL. "Biomimetic hydrogels with pro-angiogenic properties." *Biomaterials* **31** (2010): 3840-3847.

[62] Miller JS, Shen CJ, Legant WR, Baranski JD, Blakely BL, and Chen CS. "Bioactive hydrogels made from step-growth derived peg–peptide macromers." *Biomaterials* **31** (2010): 3736-3743.

[63] Van Hove AH, Beltejar M-JG, and Benoit DS. "Development and in vitro assessment of enzymatically-responsive poly (ethylene glycol) hydrogels for the delivery of therapeutic peptides." *Biomaterials* **35** (2014): 9719-9730.

[64] Van Hove AH, Antonienko E, Burke K, Brown III E, and Benoit DS. "Temporally tunable, enzymatically responsive delivery of proangiogenic peptides from poly (ethylene glycol) hydrogels." *Advanced healthcare materials* **4** (2015): 2002-2011.

[65] Goktas M, Cinar G, Orujalipoor I, Ide S, Tekinay AB, and Guler MO. "Self-assembled peptide amphiphile nanofibers and peg composite hydrogels as tunable ecm mimetic microenvironment." *Biomacromolecules* **16** (2015): 1247-1258.

[66] Jiang Y, Chen J, Deng C, Suuronen EJ, and Zhong Z. "Click hydrogels, microgels and nanogels: Emerging platforms for drug delivery and tissue engineering." *Biomaterials* **35** (2014): 4969-4985.

[67] Madl CM, and Heilshorn SC. "Bioorthogonal strategies for engineering extracellular matrices." *Advanced Functional Materials* **28** (2018): 1706046.

===

Figures and Figure Captions

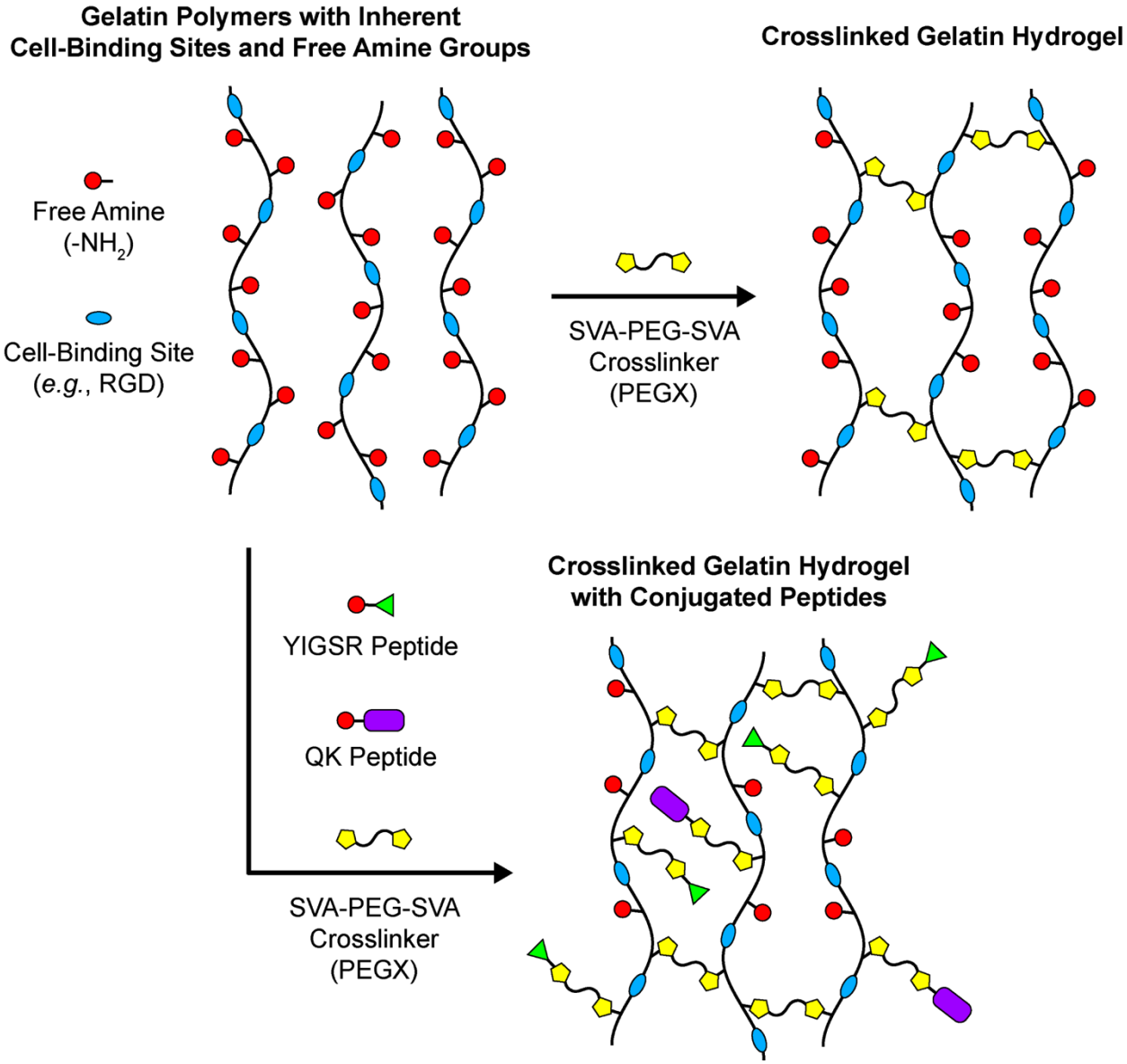

Scheme 1: Preparation of PEG-crosslinked gelatin hydrogels and conjugation of peptides. Gelatin possesses inherent cell-binding sites and free amine reactive groups. When PEGX is added to a gelatin solution, the SVA functional groups react with the free amines, forming crosslinks between gelatin polymers that results in hydrogel formation. Bioactive peptides presenting free amines, such as the YIGSR and QK peptides, can be added to the precursor polymer solution and with additional PEGX become conjugated to the gelatin polymers during hydrogel formation.

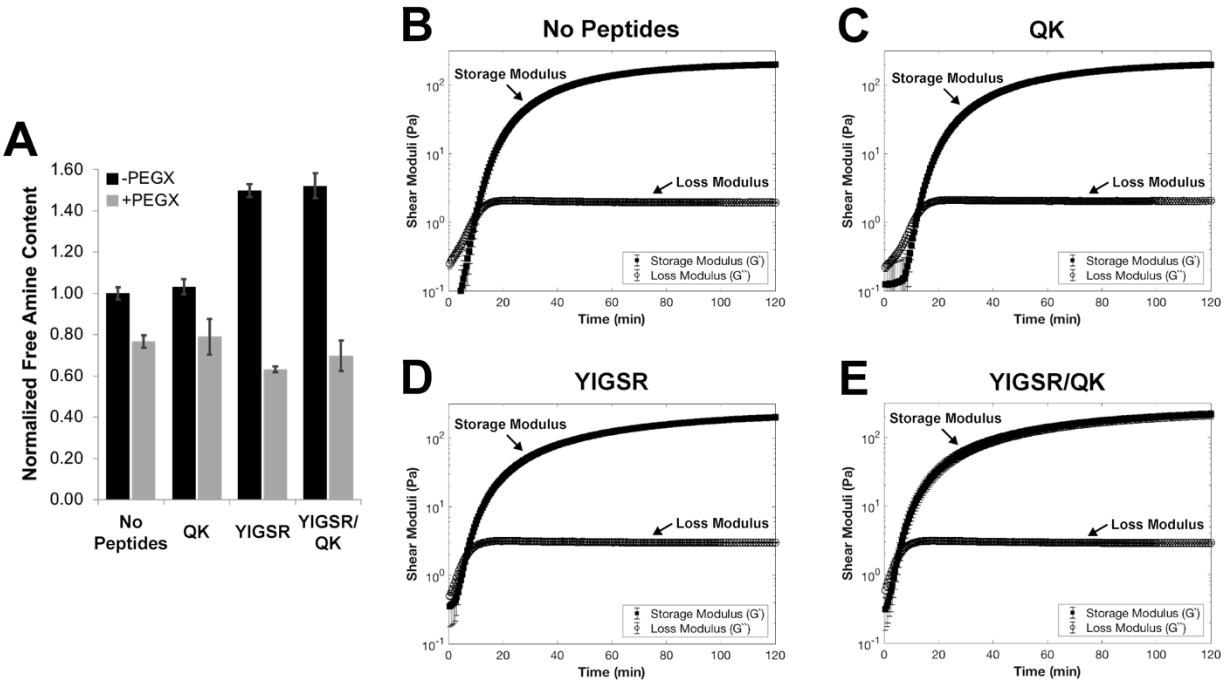

Figure 1: Quantification of free amine content and rheological time sweeps of hydrogel formulations. (A) Free amine content of uncrosslinked hydrogel precursor polymer solutions and crosslinked hydrogels quantified by the TNBS assay. Sample groups were normalized to the uncrosslinked hydrogel precursor polymer solution with no peptides group (n = 3). Rheological characterization of hydrogel formation over time with shear moduli (G', G'') plotted on semi-log plots: (B) hydrogels with no peptides, (C) QK, (D) YIGSR, and (E) YIGSR/QK hydrogels. Samples run in triplicate (n = 3).

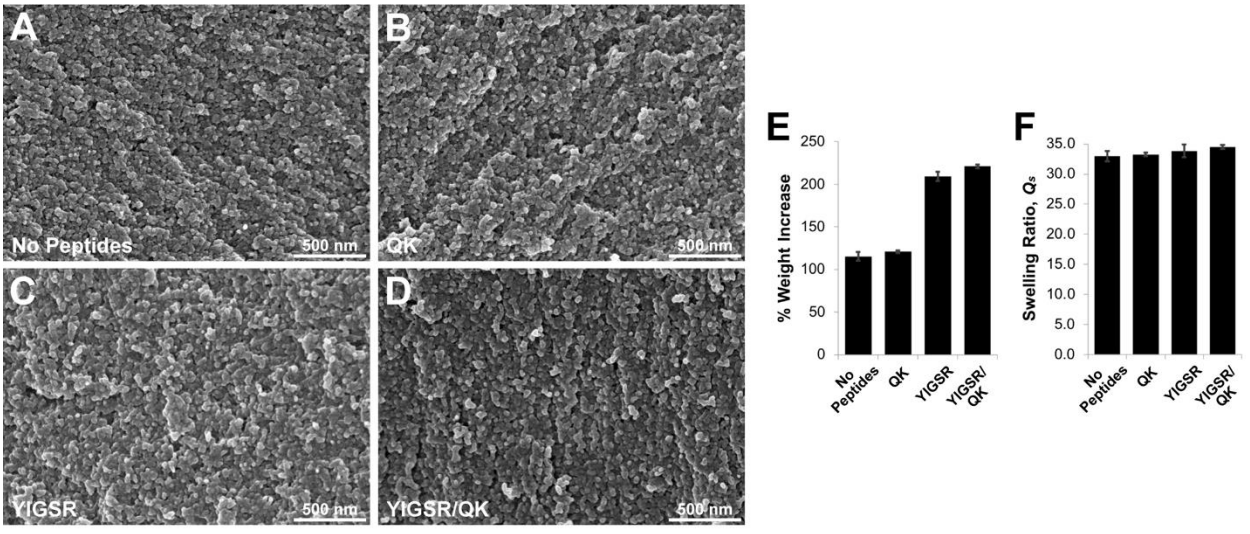

Figure 2: Scanning electron micrographs and swelling analysis of hydrogels. High-magnification scanning electron micrographs of (A) hydrogels with no peptides, (B) QK, (C) YIGSR, and (D) YIGSR/QK hydrogels. (E) Percent weight increases from initial to swollen hydrogel states, and (F) swelling ratios of swollen hydrogels to dry polymer weights (n = 6).

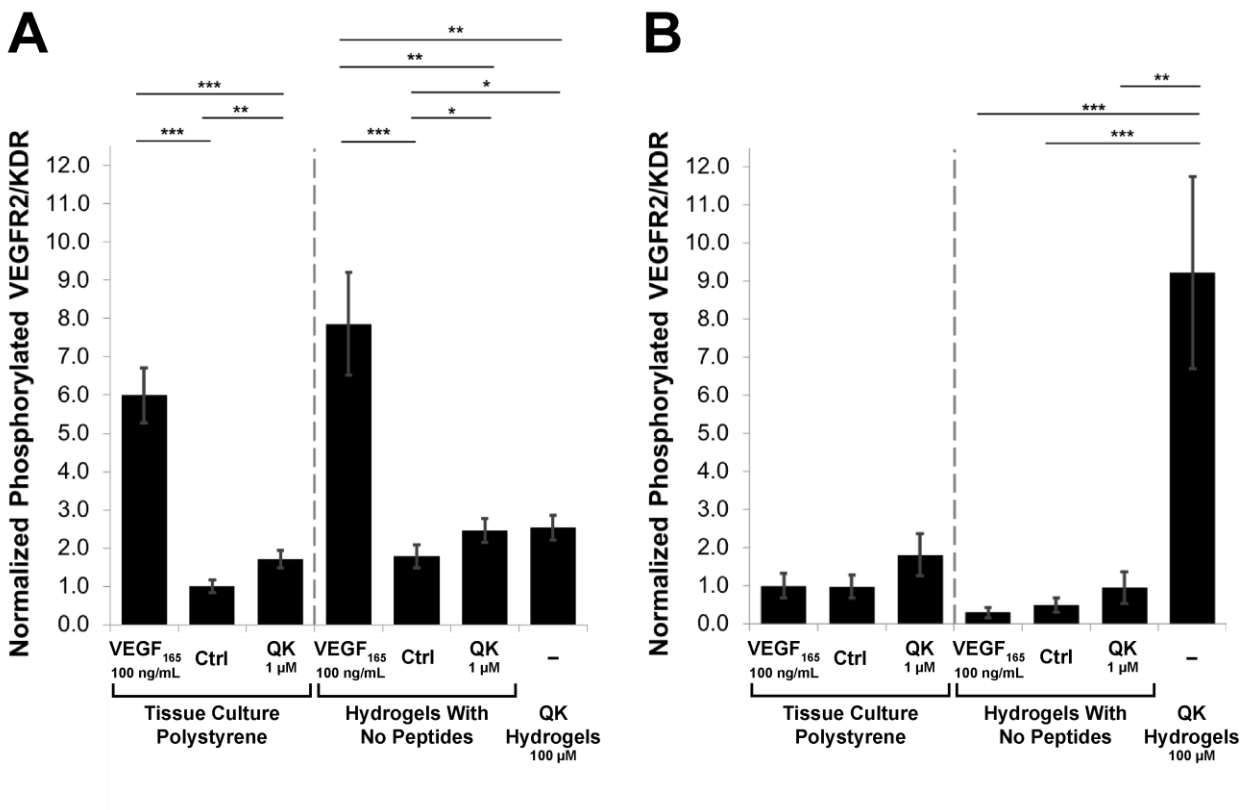

Figure 3: Cellular levels of phosphorylated VEGFR2 measured by an ELISA. Phosphorylated VEGFR2 in (A) HUVECs and (B) GEnCs following treatment with 100 ng/mL $VEGF_{165}$ (positive control), no treatment ("Ctrl", negative control), or treatment with 1 μM soluble QK peptide for cells cultured on tissue culture polystyrene or hydrogels with no peptides, or no treatment for cells cultured on QK hydrogels. Quantification was normalized to the no treatment groups on tissue culture polystyrene for each cell type (n = 4). Statistical significance denoted by: * $p < 0.05$, ** $p < 0.01$, and *** $p < 0.001$.

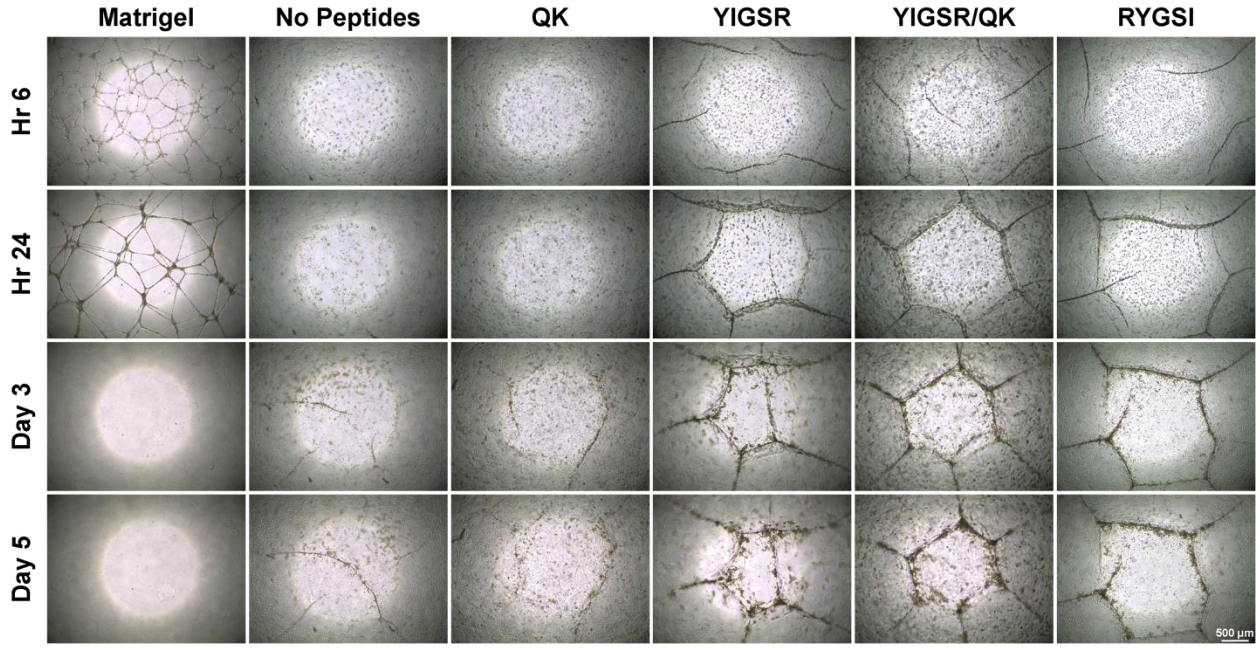

Low PPI figure to reduce file size.

Figure 4: Photomicrographs of HUVECs cultured on hydrogel substrates at designated time points showing formation of cord-like structures that vary with hydrogel formulations.

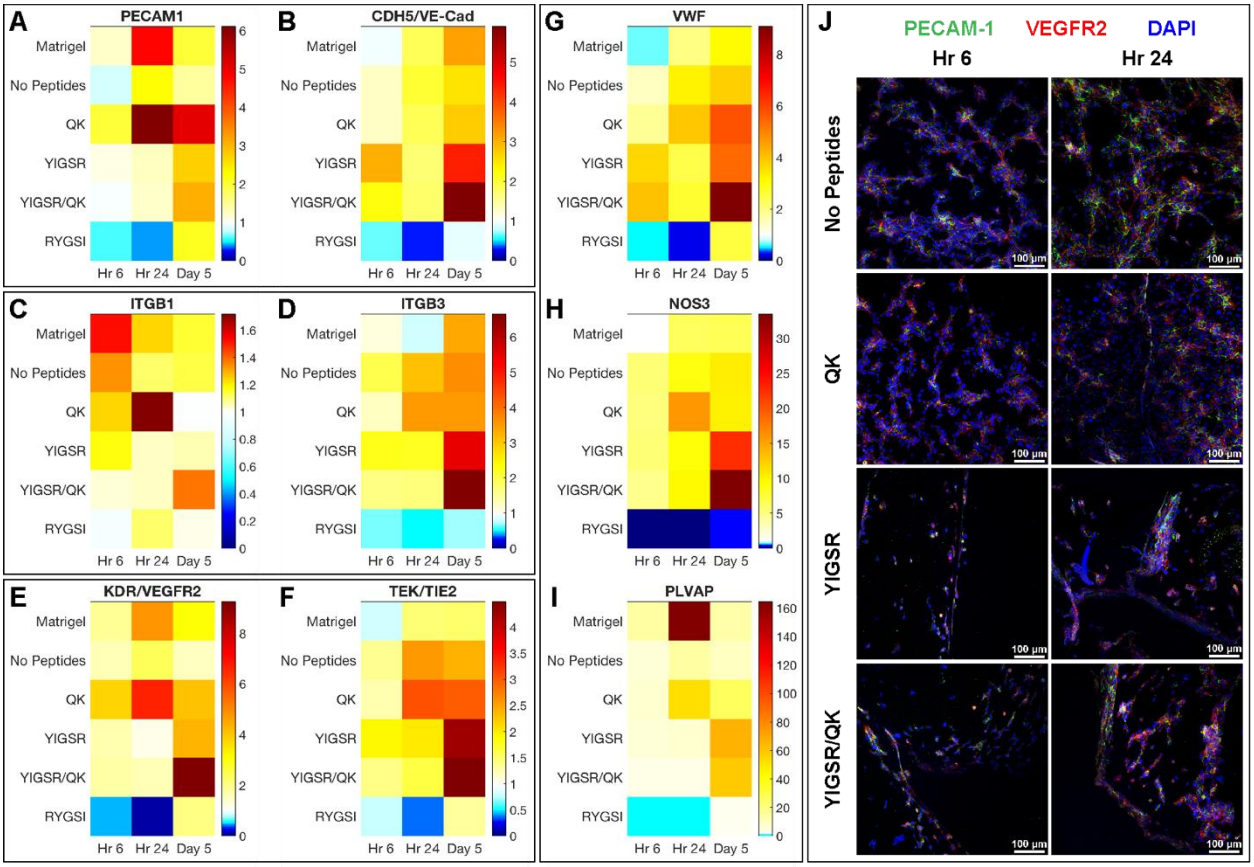

Low PPI figure to reduce file size.

Figure 5: Gene expression analysis and immunofluorescence staining of HUVECs cultured on hydrogel substrates at designated time points. (A) *PECAM1* encoding for platelet endothelial cell adhesion molecule or CD31. (B) *CDH5* encoding for cadherin 5 or vascular endothelial cadherin, also known as CD144. (C) *ITGB1* encoding for integrin subunit β1. (D) *ITGB3* encoding for integrin subunit β3. (E) *KDR* encoding for kinase insert domain receptor or vascular endothelial growth factor receptor 2. (F) *TEK* encoding for tyrosine kinase with immunoglobulin-like and EGF-like domains 2 or TIE2. (G) *VWF* encoding for von Willebrand factor. (H) *NOS3* encoding for nitric oxide synthase 3. (I) *PLVAP* encoding for plasmalemma vesicle-associated protein. Values presented as fold-change expression normalized to gene expression of HUVECs cultured in tissue culture polystyrene on day 0 (n = 4). (J) Whole-mount immunofluorescence staining of HUVECs cultured on hydrogel substrates at 6 and 24 hrs. Merged images: PECAM-1 (green), VEGFR2 (red), and DAPI (blue).

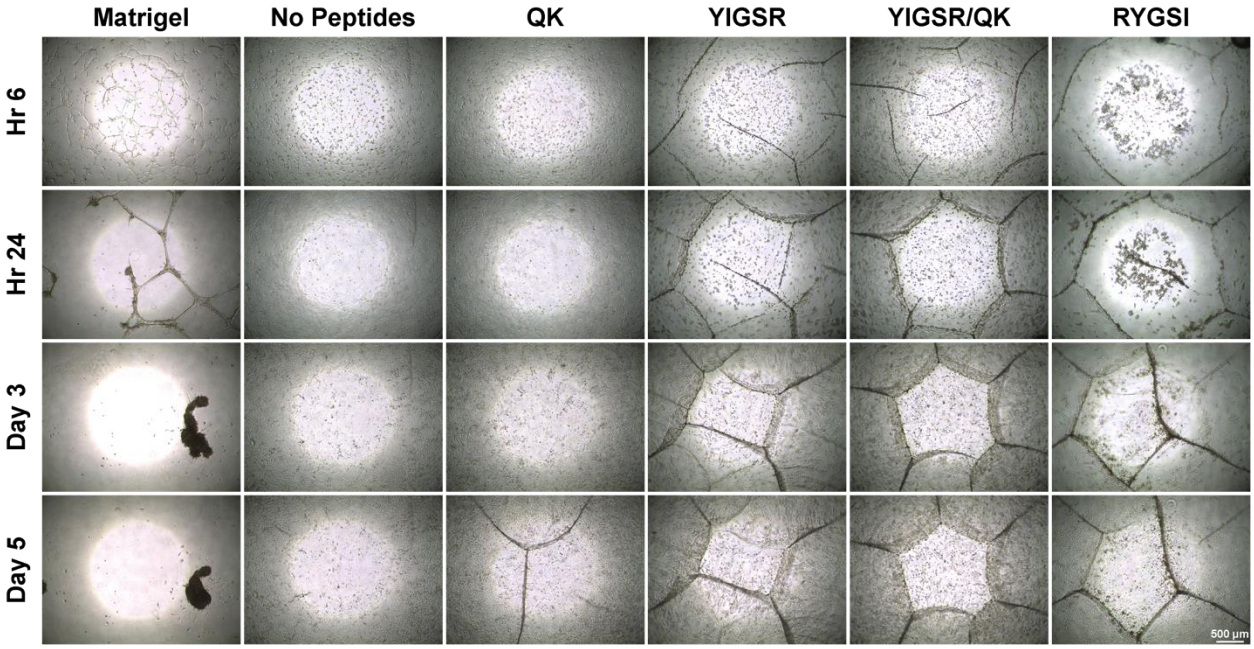

Low PPI figure to reduce file size.

Figure 6: Photomicrographs of GEnCs cultured on hydrogel substrates at designated time points showing formation of cord-like structures that vary with hydrogel formulations.

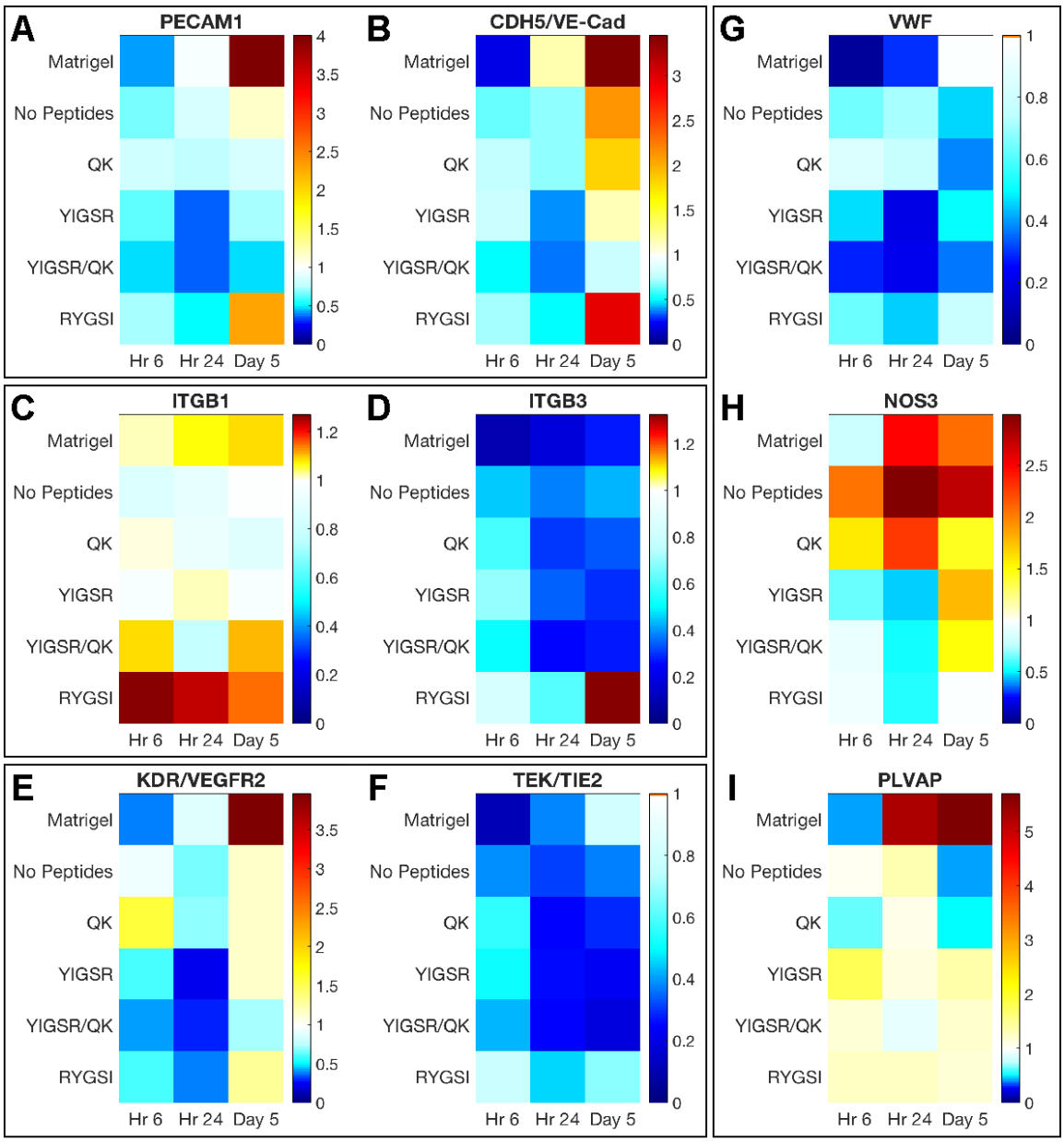

Figure 7: Gene expression analysis of GEnCs cultured on hydrogel substrates at designated time points. (A) *PECAM1* encoding for platelet endothelial cell adhesion molecule or CD31. (B) *CDH5* encoding for cadherin 5 or vascular endothelial cadherin, also known as CD144. (C) *ITGB1* encoding for integrin subunit β1. (D) *ITGB3* encoding for integrin subunit β3. (E) *KDR* encoding for kinase insert domain receptor or vascular endothelial growth factor receptor 2. (F) *TEK* encoding for tyrosine kinase with immunoglobulin-like and EGF-like domains 2 or TIE2. (G) *VWF* encoding for von Willebrand factor. (H) *NOS3* encoding for nitric oxide synthase 3. (I) *PLVAP* encoding for plasmalemma vesicle-associated protein. Values presented as fold-change expression normalized to gene expression of GEnCs cultured in tissue culture polystyrene on day 0 (n = 4).

===

===

Supplemental Figures and Figure Captions

Supplemental Table 1:
Primer Sequences for Gene Expression Analysis via Real-Time Quantitative Polymerase Chain Reaction (RT-qPCR)

Gene	Forward Primer (5' to 3')	Reverse Primer (5' to 3')
PPIA	TCG CTC TCT GCT CCT CCT GTT CGA	GGC GCC CAA TAC GAC CAA ATC C
PECAM1	TAT GAT GCC CAG TTT GAG GT	GAA TAC CGC AGG ATC ATT TG
CDH5	TTG GAA CCA GAT GCA CAT TGA T	TCT TGC GAC TCA CGC TTG AC
ITGB1	CCC ACC GTG TTC TTC GAC ATT	GGA CCC GTA TGC TTT AGG ATG A
ITGB3	GTG ACC TGA AGG AGA ATC TGC	CCG GAG TGC AAT CCT CTG G
KDR	GTG ATC GGA AAT GAC ACT GGA G	CAT GTT GGT CAC TAA CAG AAG CA
TEK	TCC GCT GGA AGT TAC TCA AGA	GAA CTC GCC CTT CAC AGA AAT AA
VWF	TGC CTC CAA AGG GCT GTA TC	CAC CAC TGT TCT CCA CTG CTC
NOS3	TGA TGG CGA AGC GAG TGA AG	ACT CAT CCA TAC ACA GGA CCC
PLVAP	CTC TTC ATG GTC TAT GGC AAC G	GCG AGC ATT CAG CCA CAT C

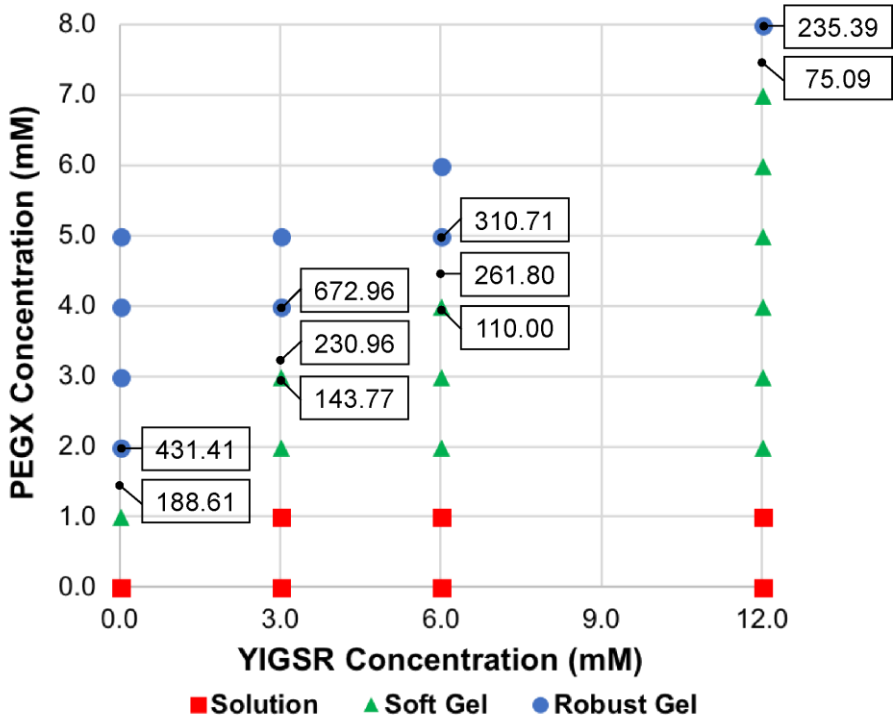

Supplemental Figure 1: Phase plot of varying YIGSR peptide concentrations with varying PEGX concentration given that the gelatin concentration is held constant at 5% (m/v). Values in boxes are the final storage moduli (in Pa) of indicated formulations as measured by two-hour time sweeps on a rheometer.

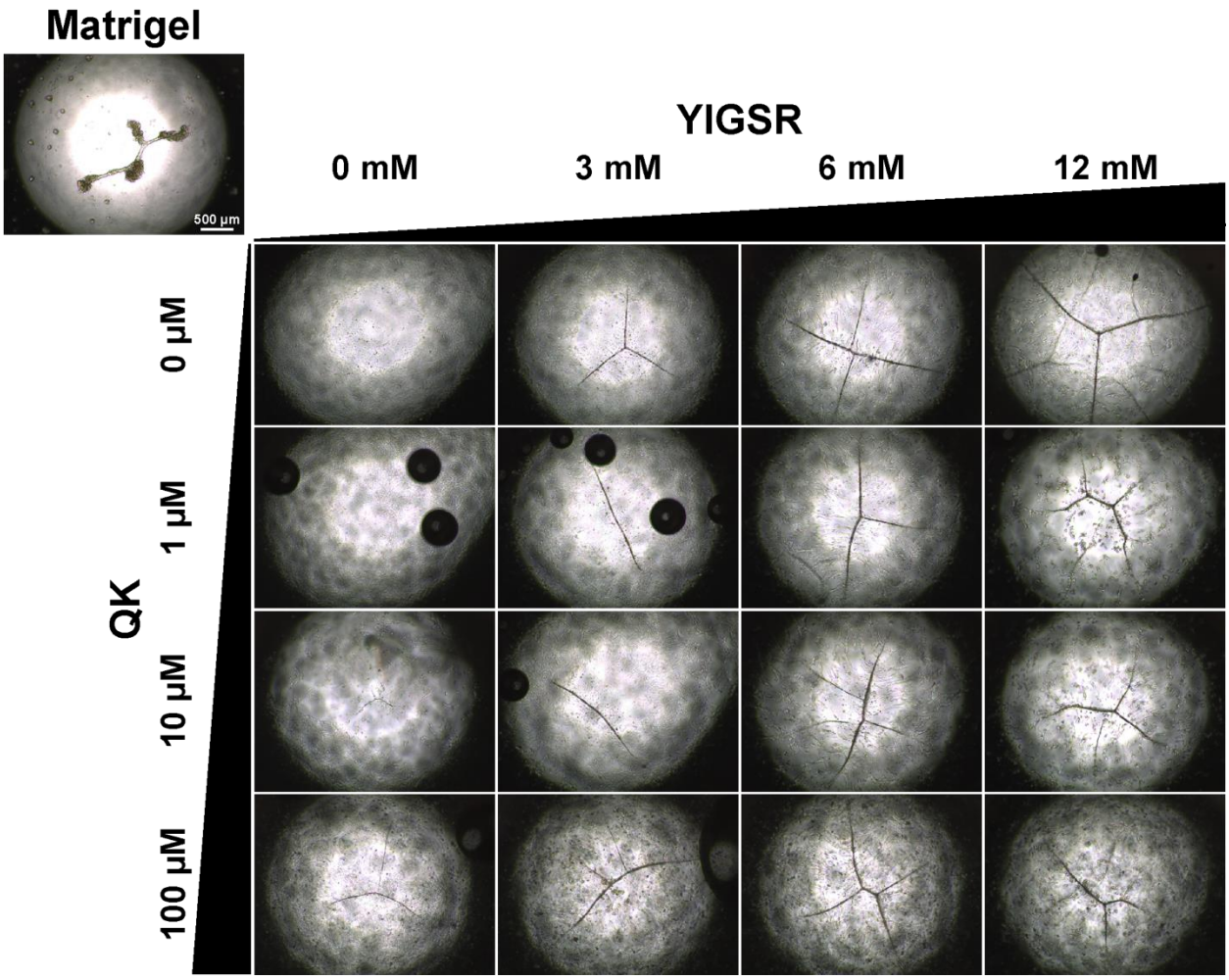

Low PPI figure to reduce file size.

Supplemental Figure 2: Photomicrographs of GEnCs cultured for 24 hrs on hydrogel substrates of varying combinations and concentrations of YIGSR and QK peptides. Matrigel was included as an additional control group.

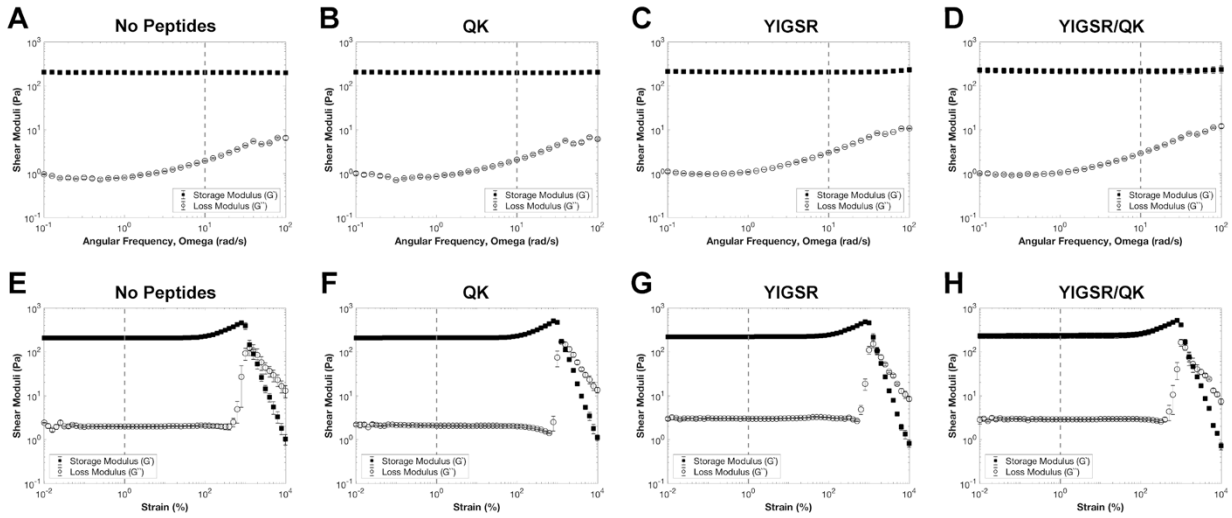

Supplemental Figure 3: Rheological frequency and strain sweeps of hydrogels. Shear moduli (*G'*, *G"*) versus angular frequency plotted on log-log plots: (A) hydrogels with no peptides, (B) QK, (C) YIGSR, and (D) YIGSR/QK hydrogels. Dashed lines represent the angular frequency at which time sweeps were performed: 10 rad/s. Shear moduli versus strain plotted on log-log plots: (E) hydrogels with no peptides, (F) QK, (G) YIGSR, and (H) YIGSR/QK hydrogels. Dashed lines represent the strain percent at which time sweeps were performed: 1% strain.

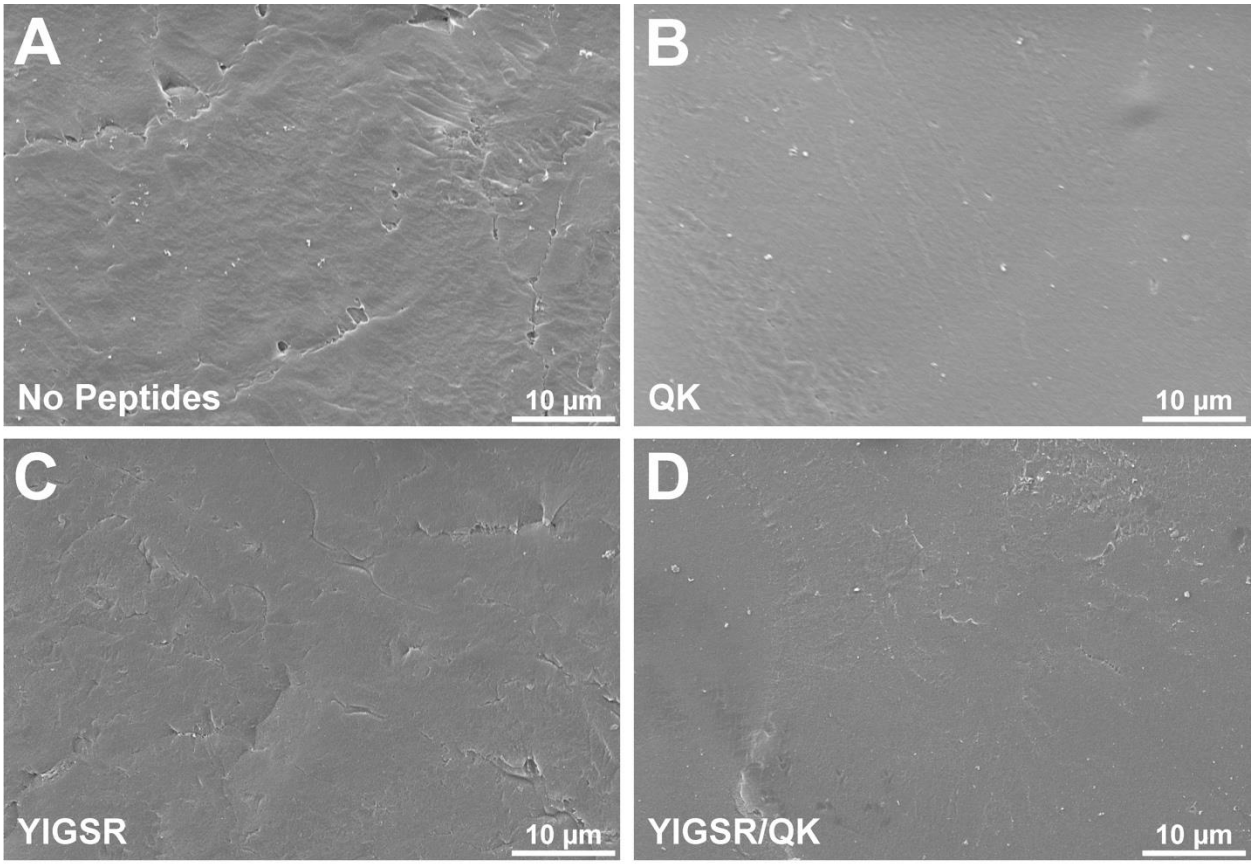

Supplemental Figure 4: Low-magnification scanning electron micrographs of hydrogels. Scanning electron micrographs of (A) hydrogels with no peptides, (B) QK, (C) YIGSR, and (D) YIGSR/QK hydrogels.